The development of molecular tools for investigating NAD+ metabolism and signalling

Minnee, H.

Chapter 4

Part of this chapter has been published:
Minnee, H., Rack, J. G. M., van der Marel, G. A., Overkleeft, H. S., Codée, J. D., Ahel, I., and Filippov, D. V., *Angew. Chem. Int. Ed.* e202313317, 2023.

Synthesis of N(π)- and N(τ)-ADP-ribosylated histidine

Introduction

Post-translational modifications (PTMs) comprise a vast collection of chemical alterations (*e.g.* methylation, phosphorylation and ubiquitination) that occur on amino acid side chains to regulate the function, localization and processing of proteins.[1] These modifications are functionally associated with a wide variety of vital biological processes such as gene expression[2], cell metabolism[3] and environmental stress responses[4] and their disruption leads to serious diseases like cancer, immune system dysfunction and neurological disorders.[3,5] Almost five decades ago, the well-known redox co-factor nicotinamide adenine dinucleotide (NAD^+) was found to be responsible for a PTM, now referred to as adenosine diphosphate (ADP)-ribosylation.[6,7] This process is primarily mediated by (ADP-ribosyl)transferases termed PARPs[8] that consume NAD^+ to construct α-glycosidic linkages on nucleophilic amino acid residues, while simultaneously expelling nicotinamide. Although the majority of PARPs introduces a single ADP-ribosyl (ADPr) molecule (mono-ADP-ribosylation or MARylation), a small subset of ADP-transferases including PARP1 and PARP2 is able to extend the chain at the 2′-OH position of the proximal ribose to generate poly-(ADP-ribose) (PAR) chains in a process termed poly-ADP-ribosylation (PARylation).[9] Branching of PAR chains occurs through the occasional elongation at the 2″-OH position of the distal ribose, giving rise to more complex secondary structures.[10] ADP-ribosylation is a fully reversible PTM due to the combined action of distinct (ADP-ribosyl)hydrolases (ARH). Cleavage of the polymer chain is mediated by poly(ADP-ribosyl)glycohydrolase (PARG)[11,12], while the removal of final protein-linked ADPr-moiety requires a collection of other hydrolases. Macrodomain proteins

can facilitate the hydrolysis of the glycosidic ester linkages of ADP-ribosylated aspartate and glutamate residues,[13,14] while cleavage of ADPr from arginine and serine residues requires ARH1[15] and ARH3[16] respectively.

The first ADP-ribosylation sites to be discovered were arginine[17,18], cysteine[19] and diphthamide,[20,21] a uniquely modified histidine residue, which were targeted by a small number of pathogenic toxins to disrupt cellular functioning. Since then, advances in mass-spectrometry (MS) have allowed for the comprehensive profiling of the 'ADP-ribosylome' to reveal the full scope of amino acid acceptors, including glutamate[22,23], aspartate[22], lysine[24], serine[25] and -as very recently discovered- tyrosine[26,27] and histidine[26,28]. It has become clear that ADP-ribosylation is a ubiquitous and highly dynamic modification that is regulated in a context specific manner by a vast network of transferases, hydrolases and ADP-interacting proteins. For example, substrate selectivity of PARP1 is directed to serine during the DNA damage response through interaction with histone PARylation factor 1 (HPF1)[29], while nicotinamide mononucleotide adenylyltransferase 1 (NMNAT-1) steers the enzymatic activity towards aspartate and glutamate residues.[23] Vital processes such as double strand DNA repair[30], inflammation[31], adipogenesis[23] and apoptosis[32] are heavily influenced by ADP-ribosylation in a direct manner and via cross-talk with other PTMs[33,23,34,35] and misfunctioning of the involved enzymes has been attributed, among others, to neurodegeneration[36], metabolic diseases[37] and impaired immune responses.[31]

Well-defined synthetic ADP-ribose oligomers and ADPr-peptides have proven to be indispensable tools to unravel the mode of action of (ADP-ribosyl) binding proteins[38,39] and hydrolases[40–42] at the atomic level and they have enabled the production of anti-ADPr antibodies[43] and standards for proteomics studies.[40] To this end, synthetic methodologies were developed that have enabled the introduction of ADP-ribose moieties on glutamine, asparagine, serine, threonine[42] and cysteine residues.[39,40,42,44] However, no methodology is available for the generation of ADP-ribosylated histidine (ADPr-His) and the exact structure of this PTM remains unknown. In line with the linkages to the other amino acid side chains and their biosyntheses,[21] the ADP-ribose moiety is most likely attached to the histidine side chain through an α-ribosyl linkage. However, the imidazolyl moiety of histidine has two potential ADP-ribosylation sites, that are commonly referred to as the N(τ)- and N(π)-position (Figure 1). It is unknown which of these or whether both regioisomers are of physiological importance and as yet, no clear transferase and hydrolase candidates have been identified for histidine ADP-ribose. As a result, there is no data available describing the exact structure of ADP-ribosyl histidine. Thus, to determine the nature of naturally occurring ADP-ribosylated histidine and study the enzymes involved in their metabolism, methodology to procure both N(τ)- and N(π)-α-ADP-ribosylated histidine peptides is desired.

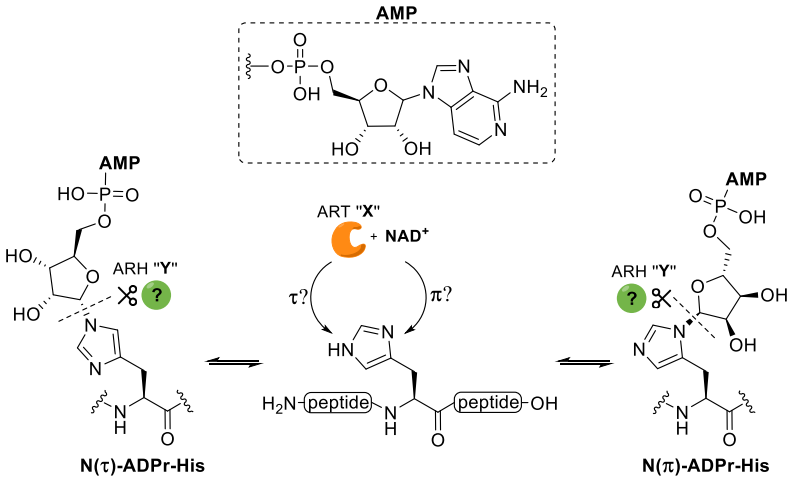

Figure 1| Schematic overview of ADP-ribosylation of histidine residues including the uncertainties surrounding the nature of this specific modification. The identity of the transferase and hydrolase involved in the construction and degradation of the PTM remain unknown and are referred to as PARP "X" and ARH "Y" respectively. NAM = nicotinamide and AMP = adenosine monophosphate.

The use of purified mammalian NADase was initially demonstrated in a series of base-exchange reactions of NAD^+ with a collection of heterocycles,[45–48] but Tono-oka and coworkers later exploited this non-specific (ADP-ribosyl)transferase-like activity to covalently attach a complete β-configured ADPr-moiety on the N(τ)-nitrogen of histidine for the very first time.[49] Despite the relevance of this enzymatic approach in preparation of ADP-ribosylated histidine, it is limited to the formation of β-configured products and thus stands in sharp contrast with the α-selectivity of known PARPs. Although there are numerous examples in literature for the, mainly β-selective, introduction of substituted imidazole groups on the anomeric position of ribofuranosides[50–53], almost no procedures towards glycosylated histidine derivatives can be found.[54,55] Only two reports describe a condensation reaction between an α-configured 1-bromopyranoside with histidine or a derivative thereof. Since glycopyranosides behave differently from their furanosyl counterparts in terms of reactivity and stereoselectivity, new and effective methodology to construct the glycosidic linkage between histidine and ADP-ribose is required. Here, the preparation of Fmoc-N^{im}-ribosylhistidine building blocks **III**, that are compatible with solid-phase peptide synthesis (SPPS), from suitably protected ribofuranosides **II** and histidine derivatives **I** using a base-assisted Mukaiyama-like glycosylation approach is described (Figure 2). The first methodology towards α-configured N(τ)- and N(π)-mono-ADP-ribosylated histidine containing peptides has subsequently been established by first implementing the modified histidine building blocks in a peptide sequence originating from histone PARylation factor 1 (HPF1), which has been identified as modification site in a recent proteomic study.[56] Then, the on-resin construction of the ADPr moiety was realized using phosphoramidite chemistry followed by a P(III)-P(V)

coupling strategy[57] with suitably protected adenosine amidites **IV**.[58] In addition, the chemical stability of the obtained α-N(τ)-, β-N(τ)- and α-N(π)-ADPr-histidine peptides under various conditions as well as their sensitivity to enzymatic digestion by (ADP-ribosyl)hydrolases were evaluated.

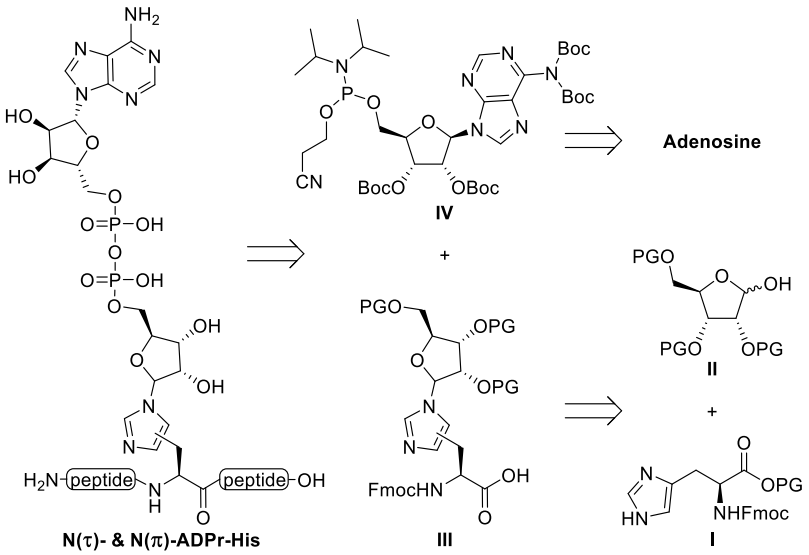

Figure 2| Retrosynthetic analysis of N(τ)- and N(π)-ADP-ribosylated histidine peptides, where PG is used to depict an unspecified protecting group.

Results and discussion

In order to synthesize ADPr-His-peptides using the general fluorenylmethyloxycarbonyl (Fmoc)-based solid-phase approach,[59] the N^{im}-ribosylated histidine building blocks had to be made accessible first. To this end, suitably protected histidine esters **3** and **5** were prepared as ribosyl acceptor in the projected glycosylation reactions. Conversion of commercially available Fmoc-His(Trt)-OH **1** into its ester derivatives (scheme 1) under basic conditions with the addition of either benzyl- or allylbromide led to disappointing yields due to the *N*-alkylation of the imidazole functionality as was observed by LC-MS analysis. Mitsunobu reaction conditions were found to be laborious and only provided the desired products in mediocre yields.[60] On the contrary, a Steglich esterification with *N,N'*-diisopropylcarbodiimide (DIC) and the corresponding alcohol efficiently provided the fully protected histidine intermediates **2** and **4** without complications. Removal of the trityl protection group could be realized by successive addition of triisopropylsilane (TIS) and trifluoroacetic acid (TFA) to the reaction mixture. Incorporation of a bicarbonate washing step during the work-up procedures is essential for isolating deprotected histidines **3** and **5** as free base instead of its TFA salt. The latter form does not only affect solubility, but more importantly reduces nucleophilic strength of the imidazole nitrogen atoms required for construction of a N-glycosidic linkage.

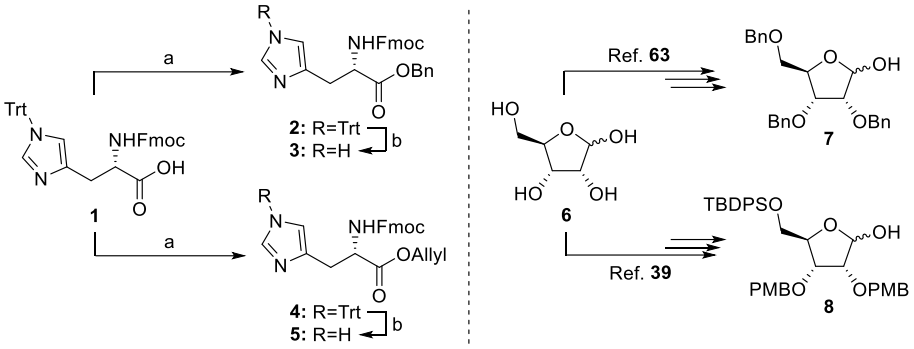

Scheme 1 | Preparation of benzyl and allyl ester derivatives of histidine **3** and **5** as glycosyl donors (left) and the derivatization of D-ribose into Mukaiyama precursors **7** and **8** (right). Reagents and conditions: a) BnOH or AllylOH, DMAP, DIC, DCM, rt, 30 min. b) TFA, TIS, DCM, rt, 16 h (94% over 2 steps for **3**, 80% over 2 steps for **5**).

Although the use of ribofuranosyl imidate donors has enabled the highly α-selective glycosylation of a variety of amino acid functionalities in the past,[39,59] no product was detected in the attempted ribosylation reaction of acceptor **3** or **5** and a ribosyl imidate donor under the aegis of catalytic or stochiometric amounts of TMSOTf. Silylation of the imidazole moiety prior to the glycosylation proved to no avail. The ensuing search for a glycosylation methodology that can operate under basic conditions led to an α-selective ribosylation reaction, introduced by Mukaiyama and co-workers,[61,62] in which an anomeric alcohol of a suitably protected ribofuranoside reacts with a diphosphonium triflate salt in the presence of a non-nucleophilic base to produce a reactive phosphonium ribosyl intermediate. The acceptor and additional base are then added to the activated donor to yield the desired ribosylated product. According to optimized conditions reported in literature,[61,62] perbenzylated model substrate **7**[63] was added with diisopropylethylamine (DIPEA) to an *in situ* prepared bis-phosphonium salt derived from tributylphosphine and triflic anhydride (Table 1). The resulting phosphonium riboside species, which could be conveniently monitored by ^{31}P NMR (94 and 98 ppm), was added to a limiting amount of benzyl ester **3** (0.6 equiv, entry 1). It quickly became apparent that both imidazole nitrogen atoms were very reactive under the given conditions since the complex mixture of isolated ribosylated histidine derivatives showed a substantial amount of doubly substituted product. Formation of the overribosylated side-product could be successfully reduced by slow addition of the activated donor solution to a two-fold excess of the acceptor over 30 min using a syringe pump (entry 2). Notably, a total of three distinct mono-substituted products were formed. Heteronuclear multiple bond correlation (HMBC) measurements demonstrated that a single anomer of N(π)-ribosylated histidine **10** was obtained alongside an inseparable anomeric mixture of N(τ)-regioisomer **9**. In view of the late stage on-resin construction of the pyrophosphate functionality, orthogonally protected ribose **8**[39] was subjected to the optimized reaction conditions

Table 1| Ribosylation of Fmoc-protected histidine analogues using diphosphonium salts. The reactions were performed at 0.5 mmol scale (limiting reagent) with final concentration of 0.013 M. Reagents and conditions: i) Bu_3PO, Tf_2O, DCE, 0 °C, 1 h. ii) **7** or **8**, DIPEA, DCE, 0 °C, 1 h. iii) **3** or **5**, DIPEA, DCE, 0 °C to rt, 16 h.

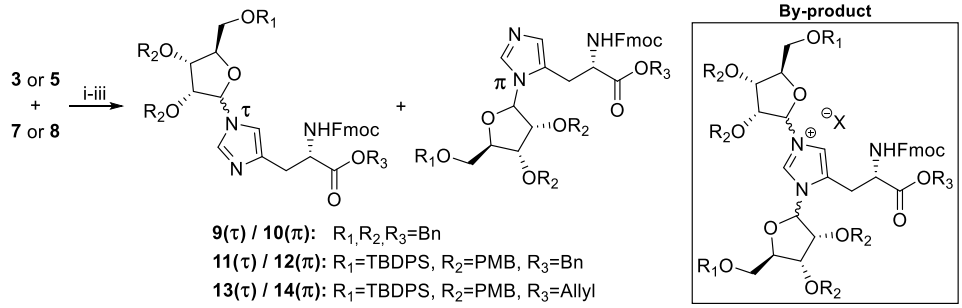

Entry	Acceptor (eq.)	Addition time $[Rib\text{-}OPBu_3]^+$	Donor (eq.)	Products	Remarks
1	**3** (1.0)	5 min	**7** (1.6)	n.d.	Significant double ribosylation
2	**3** (2.0)	30 min	**7** (1.0)	**9** (27%)*, **10** (12%)	-
3	**3** (2.0)	30 min	**8** (1.0)	**11** (32%)*, **12** (19%)	-
4	**5** (2.0)	30 min	**8** (1.0)	**13** (21%) , **14** (23%)	-
5	**5** (2.0)	30 min	**8** (1.0)	**13** (21%)*, **14** (38%)	Silylation of **5** with BSTFA
6	**5** (2.0)	60 min	**8** (1.0)	**13** (21%)*, **14** (36%)	2.5 mmol scale, 0.03 M

* double ribosylated contaminations were quantified by ^1H NMR and used to correct yields accordingly.

(entry 3). The bulky silyl protecting group on the ribose 5-OH position did not have a significant impact on the selectivity of this reaction as regioisomers **11** and **12** were acquired in a similar ratio albeit in slightly higher yields. Allyl ester **5** was also found to be compatible with the Mukaiyama-type glycosylation conditions, although for this acceptor the formation of the N(π)-substituted product **14** prevailed over its N(τ)-counterpart **13** (entry 4). Treatment of allyl ester **5** with the silylating agent BSTFA prior to addition of the activated donor (entry 5) enhanced the reactivity of the imidazolyl sidechain somewhat to provide the mixture of the three mono-ribosylated products in an improved overall yield. However, this was accompanied by an increase in di-ribosylated side products **10**, which affected the yield of the N(τ)-regioisomers **13** because of separation complications. Comparable difficulties with overglycosylation were encountered when the reaction was performed on a larger scale (entry 6). Nevertheless, ribosylated histidine analogues **8**, **9** and **11**-**14** could be consistently isolated in satisfactory yields and provided sufficient amounts to finalize the synthesis of the building blocks for Fmoc-SPPS.

Next, the benzyl ester of inseparable anomeric mixture **11** was hydrolyzed, while keeping the base-labile Fmoc group intact, using a 1.5 fold excess of lithium hydroxide at 0 °C (Scheme 2). At this stage, the two formed products showed sufficient difference in retention time to allow for careful separation by silica gel column chromatography. Although MS and NMR analysis confirmed the isolated compounds to be the N(τ)-ribosylated histidines **15** and **16**, their anomeric orientation could not be reliably established. In parallel, deallylation of epimeric mixture **13** could be efficiently mediated by palladium(0) catalysis in the presence of dimethyl barbituric acid (DMBA) as allyl scavenger to provide the N(τ)-anomers **15** and **16** in significantly higher yields than the deprotection of the corresponding benzyl ester described above. Similarly, saponification of N(π)-ribosylated benzyl ester **12** led to carboxylic acid **18** in moderate yield (47%), while the Pd(0) catalyzed deallylation of **14** provided the same product in 89% yield. Clearly the allyl ester is the preferred protection group strategy for the carboxylic acid of histidine in this synthetic endeavor.

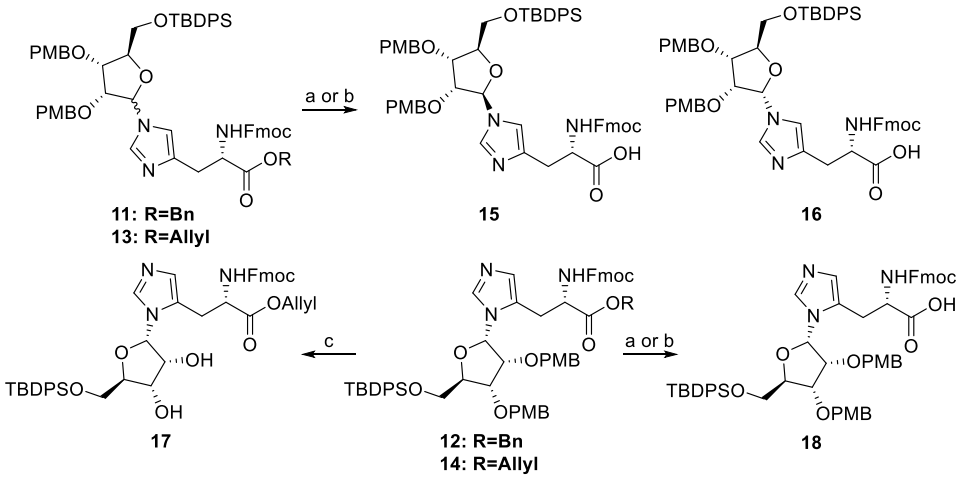

Scheme 2| Protecting group manipulations of ribosylated histidine analogues. Reagents and conditions: a) LiOH, THF/H_2O (3:1), 0 °C, 1.5 h (46% from **11**, 47% from **12**). b) $Pd(PPh_3)_4$, DCM, rt, 1 h (78% from **13**, 89% from **14**). c) HCl, HFIP, 0 °C, 10 min (36%).

Due to marginal differences in both the chemical shift and coupling constants of the anomeric proton and carbon atoms, additional NMR-spectroscopic analyses were required to elucidate the configuration of the three histidine derivatives **15**, **16** and **18**. The use heteronuclear single quantum coherence (HSQC) HECADE measurements was explored, which allows for the quantitative measurement of proton-carbon *J*-couplings (J_{CH}).[64] When the H-1 and H-2 of furanosides are *cis*-oriented the $J_{H1\text{-}C2}$ is > 0 Hertz, while *trans*-related protons show coupling constants $J_{H1\text{-}C2}$ < 0 Hertz.[65] Unfortunately, the observed coupling constants were all equal to zero and thus did not provide any clues regarding the relative orientation of H-1' and H-2'.

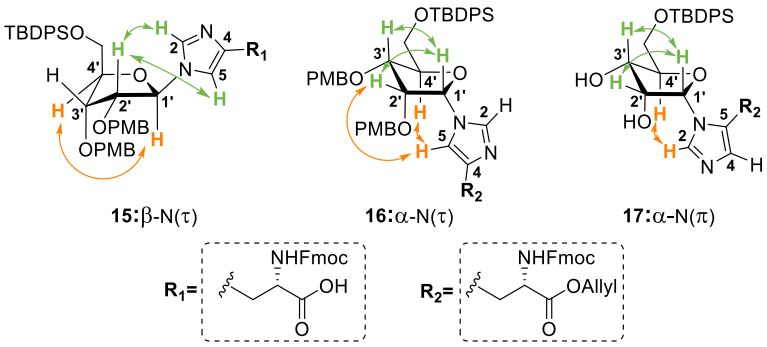

Figure 3| Schematic representation of the three ribosylated histidine analogues **15, 16** and **17** depicted in their presumed ^3E or E_3 envelope conformation, with the most relevant observed proton-proton interactions observed in NOESY measurements highlighted in red and blue. The H1′ → H2′ interaction in structure **15** has been omitted for clarity.

We therefore measured through-space interactions between the protons using nuclear overhauser effect spectroscopy (NOESY) measurements (Figure 3). In the spectra of both N(τ)-conjugated anomers **15** and **16**, a strong interaction with the neighboring H2′ could be observed. However, a signal between H-1′ and H-4′ in compound **15** indicated the imidazole functionality to have the β-configuration. This hypothesis was further substantiated by significant interactions between H-1′ and H-3′, and H-5 and H-4′ in **16**, pointing to the α-configuration of this isomer. N(π)-ribosylated carboxylic acid **18** and its allyl ester precursor **14** both displayed remarkably weak NOESY signals, so both PMB ethers were removed using a catalytic amount of HCl in HFIP[66] to provide diol **17**, which revealed clear NOESY signals. Similar to α-anomer **16**, the anomeric proton (H-1′) of **17** interacted with H-2′ as well as H-3′ while a coupling with H-4′ was lacking. In addition, an interaction of the imidazole H-2 with H-4′ supported the α-configuration of this histidine isomer.

With the configuration of all three ribosylated histidine derivatives established, their incorporation in an oligopeptide using SPPS was investigated (Scheme 3). β-Configured analogue **15** was included as a suitable negative control in later biochemical experiments. A 13 amino acid-long sequence originating from PARylation factor 1 (HPF1) presents an attractive target as the histidine residue 223 has recently been identified as an ADP-ribosylation site in recent proteomic studies.[56] Thus, the fully protected ribosylated peptides (general structure **19**) were successfully synthesized on a Tentagel resin, pre-loaded with lysine, by implementing the respective building block (**15**, **16** or **18**) through standard Fmoc-based SPPS. The TBDPS group in each of the ribosylated peptides was efficiently cleaved using HF-pyridine to liberate the primary alcohols of the immobilized ribosylpeptides (general structure **20**), after which the resin was thoroughly washed with DCM, Et_2O and finally anhydrous MeCN to remove any leftover base or water before the following steps.

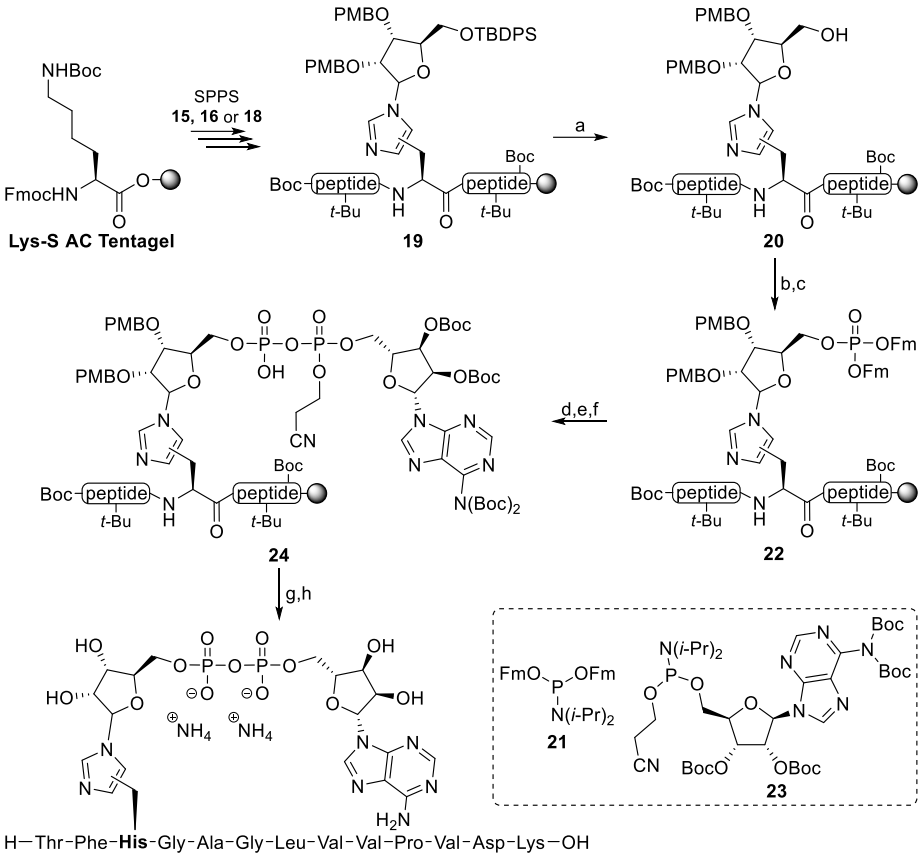

Scheme 3| Incorporation of ribosylated histidine building blocks **15, 16** and **18** and in a peptide fragment originating from HPF1. a) HF-pyridine, pyridine, rt, 2x 45 min. b) **21**, ETT, MeCN, rt, 30 min. c) CSO, MeCN, rt, 30 min. d) DBU, DMF, rt, 2x 15 min. e) **23**, ETT, MeCN, rt, 30 min. f) CSO, MeCN, rt, 30 min. g) DBU, DMF, rt, 2x 10 min. h) TFA, DCM, rt, 1 h (28% for **25**, 35% for **26** and 28% for **27** over 8 steps).

Treatment of the resin bound ribosyl peptides with the fluorenylmethyl (Fm) protected phosphoramidite **21** under the aegis of ethylthiotetrazole (ETT) as activator resulted in the phosphite triester intermediates that were immediately converted to the corresponding phosphates using (1S)-(+)-(10-Camphorsulfonyl)oxaziridine (CSO). Next, the Fm-groups of phosphates **22** were removed by treatment with dry 1,8-Diazabicyclo(5.4.0)undec-7-ene (DBU) followed by condensation with protected adenosine phosphoramidite **23**[58] through the P(III)-P(V) coupling method.[57] The coupling was directly followed by oxidation of the phosphotriester intermediate using CSO to give the immobilized protectd ADP-His peptides (general structure **24**). Elimination of the cyanoethyl group was carefully performed with DBU

followed by the global deprotection and simultaneous cleavage of the target peptides from the resin using 50% TFA in DCM. The target ADPr-histidine fragments were then purified using HPLC chromatography. The use of an ammonium acetate buffered mobile phase conveniently provided the ADP-ribosylated peptides **25-27** as stable ammonium salts, but in an inadequate purity. Fortunately, the resolution of the peaks during the HPLC purification could be sufficiently enhanced using an eluent buffered with acetic acid, allowing for the isolation of the three oligopeptides in high purity. Neutralization of the collected HPLC fractions with ammonium hydroxide before lyophilisation smoothly converted the pyrophosphates into their respective ammonium salts **25-27**.

With His-ADPr peptides **25-27** in hand, their stability under basic and acidic conditions was tested in an LC-MS based assay to evaluate their sensitivity for future synthetic and biochemical studies. A selected set of chemically diverse conditions (aqueous acid, aqueous base and a neutral nucleophile) was probed because these are commonly applied in proteomic studies to identify ADP-ribosylation sites[22] in proteins or during sample preparation.[14,28] Aqueous solutions of the ADPr peptides with a final concentration of 0.1 M TFA, 0.1 M NaOH or 0.5 M NH_2OH were prepared and shaken for 24 h at room temperature. No detectable degradation was observed for any of the peptides under the TFA and NH_2OH conditions. In contrast, the NaOH treatment led to some conversion of the N(τ)-ribosylated histidines **25** and **26** into products with an identical mass (approximately 7 and 11% respectively), indicating a slow epimerization of the modified histidine residue in N(τ)-ribosyl peptides. The base-assisted isomerization of N(π)-ADP-ribosylated peptide **27** was significantly faster and was therefore monitored in a follow-up time-course experiment (Figure 4A). After 24 h, no more isomerization is observed, leading to a mixture in which approximately 60% of the ADPr-peptide remains in its original form. No cleavage of the *N*-glycosidic bond of the distal ribose has been observed in any of the samples, which is in correspondence to the stability described for glucopyranosylimidazoles under both acidic and basic conditions.[67] The stability of ADPr-His to aqueous hydroxylamine and acid and the sensitivity of it to base-catalyzed epimerization effectively parallels the behavior of the triazole-based isosteres of ADPr-His described in Chapter 2 and 3. These chemical similarities supports the idea that the latter are indeed a suitable substitute for ADPr-His at least in some respects. It is noteworthy that even after a week of alkaline treatment, no degradation of the pyrophosphate linkage was observed. Combined with earlier findings,[40] this suggests that the pyrophosphate in the mono-ADPr-conjugates is stabilized by the peptide backbone and only becomes susceptible to nucleophilic degradation once it has been eliminated from the amino acid residue. With the chemical stability of peptides **25-27** established, it was probed whether any of the so-far identified human (ADP-ribosyl)hydrolases has the ability to catalyze the turnover of the histidine modifications (Figure 4B).

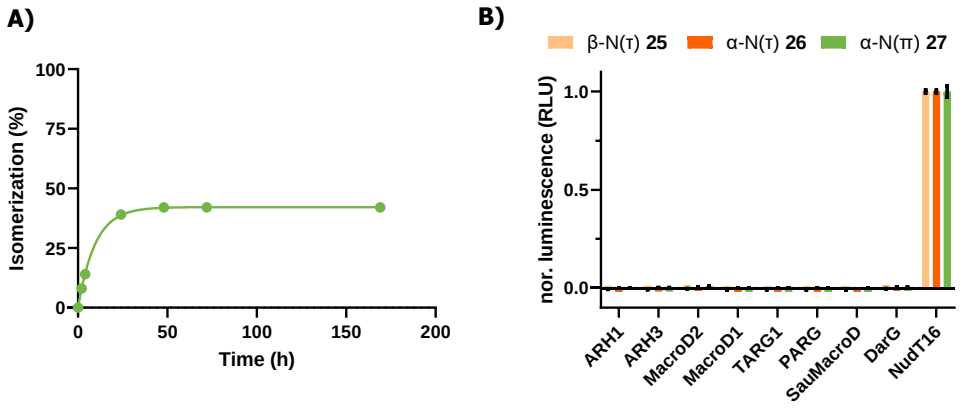

Figure 4 | A. Chemical stability of peptide **27** under basic conditions (NaOH, 0.1 M). Samples were extracted at different time points (2, 4, 24, 48, 72 and 169 h) and quenched with TFA prior to LC-MS injection. Peptide degradation was quantified by analyzing the UV-trace (260 nm) using Xcalibur software. Including an exponential one-phase decay trendline (Y=42.2*e(-0.1024*X)+57.8, R^2 = 0.999). B. Enzymatic hydrolysis of interglycosidic linkages in ADP-ribosylated histidine peptides **25-27**. Enzymatic turnover of the various peptides was assessed by monitoring AMP release directly (NudT16) or converting released ADPr via NudT5 to AMP. AMP was measured using the AMP-Glo assay (Promega). Samples are background corrected and normalized to NudT16 activity.

To this end peptides **25-27** were incubated with different (ADP-ribosyl)hydrolases in combination with Nudix hydrolase (NudT) 5. The former hydrolases have been shown to cleave mono-ADP-ribose moieties from aspartic acid and glutamic acid (MacroD1, D2 and TARG1), arginine (ARH1) serine (ARH3),[68] cysteine (*Sau*MacroD[59]) and ADP-ribosylated DNA modified at the N-3 position of a thymidine (TARG[69] and *Taq*DarG[70]) or N-2 position of a guanosine base (*Cdn*NADAR[71]), while NudT5 transforms the liberated ADPr into adenosine monophosphate (AMP) that allows for the quantification of hydrolase activity using the commerical AMP-Glo assay.[40] Luminescent signals are normalized against a positive control where the sample is incubated with NudT16, an enzyme capable of the hydrolysis of the pyrophosphate linkage of both free and bound ADPr.[72] Surprisingly, none of the tested hydrolases are capable of cleaving the ADPr-modification on any of the three peptides, while hydrolysis of triazolyl-based ADP-ribosylated HPF1 conjugates (generated by a click reaction between an 1''-azido-ADP-ribose with a suitable peptide alkyne and representing a close mimic of the putative natural substrate, Chapter 2 and 3) has been observed for ARH3.[73] The sensitivity of the latter ADPr-triazoles to ARH3 *in vitro* probably results from a combination of the relative promiscuity in hydrolase activity of ARH3 and the good leaving group capacity of the triazolide anion (pKa (1,2,3-triazole) = 9.4 versus pKa (imidazole) = 14.5). The high chemical and enzymatic stability of ADP-ribosylated histidine, on the one hand, may suggest irreversibility of this PTM and, on the other hand, invites the search for the yet unidentified enzyme(s) capable of cleaving the ADPr-histidine linkage. The tools generated here will be instrumental in this quest. At the same time, at present no definite conclusions can be drawn

about the structure of ADP-ribosylated histidine residues, regarding the modification site on the histidine imidazole ring.

Conclusion

A novel methodology for solid-phase synthesis of α-configured ADP-ribosylated histidine peptides has been developed for the first time. The synthetic well-defined ADPr-His-peptides will assist in determining the exact structure of this modification and may enable the discovery of hydrolases that can reverse ADP-ribosylation of histidine in the living organisms as well as proteins containing macrodomains capable of binding ADPr-His specifically. The synthesis of the desired ribosylated building blocks α-N(τ) **16** and α-N(π) **18** was realized through a modified Mukaiyama glycosylation reaction using a suitable protected *in situ* generated phosphonium ribofuranoside donor. The exact structure of three key ribosyl histidine intermediates was elucidated using HMBC and NOESY measurements. The desired ADPr-peptides **25-27** were generated using standard Fmoc-based SPPS combined with effective P(III)-P(V) pyrophosphate chemistry. The histidine ADPr PTM proved to be rather stable under both chemical (acidic, nucleophilic and basic) conditions as well as enzymatic degradation conditions. Strikingly, none of the known human (ADP-ribosyl)hydrolases (ARH) have the ability to cleave ADPr-His. These findings are all the more striking, considering the extensive substrate spectrum of ARH3 (including α-NAD^+,[74] poly-ADPr,[75] O-acetyl-ADPr,[76] ADPr-Ser,[40] ADPr-5'P DNA[77] and ADPr-triazolyl conjugates[73]), and suggest the existence of a yet unidentified enzyme with (ADP-ribosyl)hydrolase activity towards histidine. The newly synthesized molecular tools will be of great value in the discovery of these enzymes and well as uncovering new macrodomains capable of reading the ADPr code.

Experimental section

General synthetic procedures

Glycosyl donors 2,3,5-tri-*O*-benzyl-D-ribofuranose **7**[63] and 5-TBDPS-2,3-bis-*O*-PMB-D-ribofuranose **8**[39] were synthesized, over 3 and 4 steps respectively, from D-ribofuranose according to previously reported procedures. All chemicals were used as received unless stated otherwise. Dowex 50WX8 hydrogen form (100-200 mesh) was purchased at Sigma Aldrich and washed with H_2SO_4 (5 M, 3x) and MeOH (3x) prior to use. Molecular sieves were flamedried (3x) in vacuo before use. Solvents were dried over activated 4Å molsieves for 24 h except for MeCN and MeOH which were dried over 3Å molsieves. A solution of HCl (0.2 M in HFIP) was freshly prepared prior to the reaction by dissolving HCl (37%, 0.1 ml) to HFIP (5.9 ml). Reactions were performed under N_2 atmosphere unless stated otherwise. A Julabo FT902 cryostat was used for low temperature glycosylation reactions. Reaction mixtures were concentrated under reduced pressure using rotary evaporators at 40-45 °C unless state otherwise. Reactions were monitored by thin layer chromatography (TLC) analysis using silica gel 60 F254 coated aluminum sheets from Merck. TLC plates were visualized with ultraviolet light (254 nm) or sprayed with H_2SO_4 (20% v/v in MeOH), potassium permanganate (1 g $KMnO_4$, 5 g K_2CO_3, in 200 ml H_2O) or ceric ammonium molybdate (1 g $Ce(NH_4)_4(SO_4)_4 \bullet 2H_2O$, 2.5 g $(NH_4)_6Mo_7O_{24} \bullet 4H_2O$, 10 ml H_2SO_4 in 90 ml H_2O). Infrared (IR) values are reported in cm^{-1}. ^1H NMR, ^{13}C NMR and ^{31}P NMR spectra were recorded on Bruker AV-300 (300 mHz), AV-400 (400 mHz) or AV-500 (500 mHz) spectrometer. ^{13}C NMR spectra are acquired via the attached proton test (APT) experiment and are presented with even signals (C_q and CH_2) pointing upwards and odd signals (CH and CH_3) pointing downwards. The chemical shifts are noted as δ-values in parts per million (ppm) relative to the tetramethylsilane signal (δ = 0 ppm) or solvent signal of D_2O (δ = 4.79 ppm) for ^1H NMR and relative to the solvent signal of $CDCl_3$ (δ = 77.16 ppm) for ^{13}C NMR. Phosphorylation reactions were monitored with ^{31}P NMR using an acetone-D_6 insert for a locking signal and the resulting spectra were indirectly calibrated with H_3PO_4. HRMS samples were prepared in either MeOH, MeCN or milliQ grade H_2O with an approximate concentration of 1 mM and measured on a Thermo Scientific LTQ Orbitrap XL.

Solid phase peptide synthesis

Fmoc-Asp(*t*-Bu)-OH, Fmoc-Val-OH, Fmoc-Pro-OH, Fmoc-Leu-OH, Fmoc-Gly-OH, Fmoc-Ala-OH and Fmoc-Phe-OH were all obtained from Merck Novabiochem. Boc-Thr(tBu)-OH was acquired from BLD pharmatech GmbH. Lysine(Boc) was purchased pre-loaded on tentagel® S AC resin from RAPP Polymere GmbH.

The Fmoc-N-Ala-Gly-Leu-Val-Val-Pro-Val-Asp-Lys-S AC linked Tentagel® sequence was prepared using a Liberty Blue peptide synthesizer via 9-fluorenylmethoxycarbonyl (Fmoc) based solid phase peptide chemistry at a 250 µmol scale. A 4 fold excess of the amino acids relative to the resin loaded amino acid was added in each prolongation step. A total of 4 equivalents of the additives Diisopropylcarbodiimide (DIC) and OxymaPure were added simultaneously. The coupling was established in the microwave reaction chamber at 90 °C for 2.5 minutes. After each coupling the peptide was subjected three consecutive times to a 20 v/v% piperidine solution in DMF at 90 °C for 1 minute to remove the Fmoc protection group.

The Fmoc-N-Ala-Gly-Leu-Val-Val-Pro-Val-Asp-Lys-Tentagel® sequence was completed at a 50 µmol scale by hand in a fritted syringe. After each step the resin was rinsed with the corresponding solvent (3x 3 ml) unless stated otherwise. Fmoc proctecting groups were removed by treatment with piperidine twice (10v/v% in DMF, 3 ml) for 3 and 7 min. Ribosylated amino acids **15**, **16** or **18** (0.1 mmol, 2 eq.) were coupled overnight in the presence DIPEA (40 µl, 4.5 eq.) and HCTU (0.1 mmol, 2 eq.) in DMF (3 ml).

Fmoc-Phe-OH and Boc-Thr(*t*-Bu)-OH (0.25 mmol, 5 eq) were coupled for 45 min with HCTU (0.25 mmol, 5 eq) and DIPEA (90 µl, 10 eq.) in DMF (3 ml).

On-resin phosphorylation, pyrophosphate construction and final deprotection

TBDPS deprotection was achieved by treating the resin (50 µmol) with HF-pyridine (70 wt%, 1 ml) in pyridine (3 ml) twice for 45 min. The resin was washed with DMF (3x 3ml), DCM (3x 5 ml), Et_2O (3x 5 ml) and anhydrous MeCN (3x 3 ml) and flushed with nitrogen to minimize traces of water. Subsequently, the desilylated intermediate was treated with Fm-protected amidite **21** (0.25 mmol, 5 eq.) and ETT (0.25 mmol, 5 eq.) in anhydrous MeCN (3 ml) for 30 min. CSO (1 mmol, 20 eq.) in anhydrous MeCN (2 ml) was added and the resin was shaken again for 30 min. Then the newly introduced phosphate was deprotected with DBU (10v/v% in DMF, 2 ml) twice for 15 min and thoroughly washed with DCM (3x 5 ml), Et_2O (3x 5 ml) and anhydrous MeCN (3x 3 ml) before treating with **23**[58] (0.2 mmol, 4 eq.) in the presence of ETT (0.4 mmol, 8 eq.) in anhydrous MeCN (3 ml) for 30 min. The P(III)-P(V) intermediate was oxidized again with CSO (1 mmol, 20 eq.) in anhydrous MeCN (2 ml) for 30 min. The resin was subsequently shaken with DBU (10v/v% in anhydrous DMF, 2 ml) twice for 10 min each to remove the cyanoethyl group. The modified oligopeptide was cleaved from the resin using TFA/TIS/DCM (50:50:2.5, 4 ml) for 1 h. The solution was poured into a Falcon® tube containing ice cold Et_2O (45 ml) and the resulting suspension was centrifuged (5 min, 3000 RCF) using an Eppendorf centrifuge 5702 followed by removal of the supernatant. The crude residues were neutralized with NH_4OH (28wt% in H_2O), lyophilized and subjected to preparative RP-HPLC (AcOH buffered system). Product fractions were collected and neutralized with NH_4OH (28wt% in H_2O) prior to lyophilisation to yield the desired peptide conjugate as ammonium salt.

Fmoc-His-OBn (3).

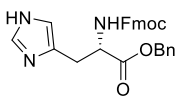

Fmoc-His(Trt)-OH (19.7 g, 31.8 mmol), DMAP (0.39 g, 3.2 mmol) and benzyl alcohol (5.0 ml, 48 mmol) were dissolved in anhydrous DCM (160 ml). DIC (7.4 ml, 48 mmol) was added and the clear solution was stirred at rt for 30 min. For analytical purposes, a small sample was concentrated under reduced pressure and purified by silica gel column chromatography (pentane/EtOAc = 95:5 → 80:20) to yield **2** as a white solid. $\mathbf{R_f}$ = 0.3 (pentane/Et_2O = 50:50) HUM337 **^{1}H NMR** (400 MHz, $CDCl_3$): δ 7.75 (d, *J* = 7.5 Hz, 2H), 7.62 (t, *J* = 6.8 Hz, 2H), 7.42 – 7.19 (m, 14 H), 7.14 – 7.05 (m, 6H), 6.61 (d, *J* = 8.2 Hz, 1H), 6.50 (d, *J* = 1.4 Hz, 1H), 5.05 (q, *J* = 12.2 Hz, 2H), 4.72 – 4.63 (m, 1H), 4.40 – 4.19 (m, 3H), 3.08 (dd, *J* = 5.0, 2.9 Hz, 2H). **^{13}C NMR** (101 MHz, $CDCl_3$): δ 171.5, 156.3, 144.2, 144.0, 142.3, 141.3, 141.3, 138.9, 136.4, 135.5, 129.8, 128.6, 128.3, 128.2, 128.1, 127.7, 127.7, 127.1, 127.1, 125.5, 125.4, 119.9, 119.7, 75.4, 67.3, 66.9, 54.4, 47.2, 30.1. **HRMS** $[C_{47}H_{40}N_3O_4 + H]^+$ = 710,30028 found, 710,30133 calculated.

Then TFA (22 ml, 286 mmol) and TIS (9.8 ml, 48 mmol) were added and the reaction mixture was stirred at rt overnight. The yellow solution was concentrated under reduced pressure. and co-evaporated with toluene (3x). Purification of the crude residue by silica gel column chromatography (DCM/MeOH = 97.5:2.5→ 90:10) provided title compound **3** as TFA salt. The white solid was dissolved in $CHCl_3$/*i*-PrOH (4:1 v/v, 400 ml), washed with $NaHCO_3$ (sat., 2x 200 ml) and brine (200 ml). The organic fraction was dried over $MgSO_4$, filtered and concentrated under reduced pressure to yield title compound **3** (14 g, 29.9 mmol, 94% over 2 steps) as a white foam. $\mathbf{R_f}$ = 0.25 (DCM/MeOH = 95:5). **^{1}H NMR** (400 MHz, $CDCl_3$): δ 7.71 (d, *J* = 7.6 Hz, 2H), 7.54 (dd, *J* = 7.6, 4.7 Hz, 2H), 7.45 (s, 1H), 7.35 (s, 1H), 7.30 – 7.19 (m, 7H), 6.57 (s, 1H), 6.45 (d, *J* = 8.0 Hz, 1H), 5.16 – 5.05 (m, 2H), 4.69 – 4.61 (m, 1H), 4.37 – 4.24 (m, 2H), 4.17 (t, *J* = 7.3 Hz, 1H), 3.11 (d, *J* = 5.4 Hz, 2H). **^{13}C NMR** (101 MHz, $CDCl_3$): δ 171.6, 156.3, 143.9, 143.8, 141.2, 141.2, 135.5, 135.4, 135.3, 133.8, 128.8, 128.6, 128.6, 128.5, 128.4, 128.4, 128.4, 128.3,

127.7, 127.2, 127.1, 125.2, 125.2, 124.9, 121.0, 120.0, 119.8, 116.1, 107.8, 77.3, 67.3, 67.2, 67.1, 66.9, 54.3, 47.1, 29.5. **HRMS** $[C_{28}H_{25}N_3O_4 + H]^+$ = 468.19146 found, 468,19178 calculated.

Fmoc-His-OAllyl (5).

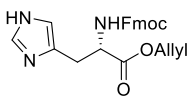

Fmoc-His(Trt)-OH (25 g, 40.3 mmol), DMAP (0.49 g, 4.0 mmol) and allyl alcohol (5.5 ml, 81 mmol) were dissolved in anhydrous DCM (134 ml). DIC (6.9 ml, 44 mmol) was added and the clear solution was stirred at rt for 30 min. For analytical purposes, a small sample was concentrated under reduced pressure and purified by silica gel column chromatography (pentane/EtOAc = 90:10 → 70:30) to yield **4** as a white solid. $\mathbf{R_f}$ = 0.5 (pentane/Et_2O = 50:50) HUM376-2 **^{1}H NMR** (400 MHz, $CDCl_3$): δ 7.72 (d, *J* = 8.0 Hz, 2H), 7.66 – 7.57 (m, 2H), 7.43 (d, *J* = 1.4 Hz, 1H), 7.39 – 7.22 (m, 13H), 7.15 – 7.06 (m, 6H), 6.73 (d, *J* = 8.3 Hz, 1H), 6.59 (d, *J* = 1.4 Hz, 1H), 5.78 (ddt, *J* = 17.3, 10.4, 5.7 Hz, 1H), 5.21 (dd, *J* = 17.2, 1.5 Hz, 1H), 5.10 (dd, *J* = 10.4, 1.3 Hz, 1H), 4.68 (dt, *J* = 8.3, 4.9 Hz, 1H), 4.59 – 4.43 (m, 2H), 4.43 – 4.15 (m, 3H), 3.11 (t, *J* = 4.5 Hz, 2H). **^{13}C NMR** (101 MHz, $CDCl_3$): 171.2, 156.2, 144.0, 143.8, 142.2, 141.1, 141.1, 138.8, 136.3, 131.7, 129.6, 128.0, 128.0, 127.5, 127.0, 127.0, 125.3, 125.2, 119.8, 119.5, 118.4, 77.3, 75.2, 67.1, 65.6, 54.2, 47.0, 30.0. **HRMS** $[C_{43}H_{37}N_3O_4 + H]^+$ = 660.28518 found, 660.28568 calculated.
Then TFA (31.1 ml, 403 mmol) and TIS (12.4 ml, 60.5 mmol) were added and the reaction mixture was stirred at rt overnight. The yellow solution was diluted with DCM (200 ml) and washed with $NaHCO_3$ (sat., 4x 200 ml). The H_2O layer was back-extracted with DCM (1x 100 ml). The combined organic fractions were dried over $MgSO_4$, filtered and concentrated under reduced pressure Purification of the crude residue by silica gel column chromatography (DCM/Acetone = 100:0 → 50:50, 10% steps) provided title compound **5** (13.5 g, 32.3 mmol, 80% over 2 steps) as a white foam. $\mathbf{R_f}$ = 0.3 (DCM/MeOH = 95:5). **^{1}H NMR** (400 MHz, $CDCl_3$): δ 7.73 (d, *J* = 7.6 Hz, 2H), 7.60 – 7.50 (m, 2H), 7.37 (t, *J* = 7.5 Hz, 2H), 7.27 (t, *J* = 7.5 Hz, 2H), 6.77 (s, 1H), 6.37 (d, *J* = 7.5 Hz, 1H), 5.83 (ddt, *J* = 16.5, 11.0, 5.7 Hz, 1H), 5.29 – 5.14 (m, 2H), 4.63 (q, *J* = 6.3 Hz, 1H), 4.57 (d, *J* = 5.8 Hz, 2H), 4.33 (p, *J* = 10.5 Hz, 2H), 4.20 (t, *J* = 7.4 Hz, 1H), 3.14 (d, *J* = 5.5 Hz, 2H). **^{13}C NMR** (101 MHz, $CDCl_3$): 171.5, 156.3, 143.9, 143.8, 141.3, 141.3, 135.3, 134.2, 131.6, 127.7, 127.1, 125.2, 120.0, 118.7, 115.9, 67.2, 66.0, 54.3, 47.2, 29.6. **HRMS** $[C_{24}H_{23}N_3O_4 + H]^+$ = 418.17606 found, 418.17613 calculated.

Fmoc-His(1′-N(τ)-2′,3′,5´-tris-*O*-benzyl-D-ribofuranosyl)-OBn (9) and Fmoc-His(1′-N(π)-2′,3′,5´-tris-*O*-benzyl-D-ribofuranosyl)-OBn (10).

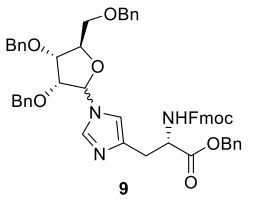

9

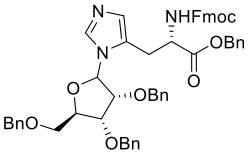

10

Bu_3PO (535 mg, 2.45 mmol) was co-evaporated with toluene (3x), dissolved in anhydrous DCE (10 ml) and cooled to 0 °C. Tf_2O (1 M, 1.15 ml, 1.15 mmol) was added dropwise over 20 min using a syringe pump and the resulting pinkish solution was stirred for 1 h at 0 °C. ^{31}P NMR indicated formation of the diphosphonium salt (δ = 119.5 ppm). **7** (0.21 g, 0.50 mmol) was co-evaporated with toluene (3x), dissolved in anhydrous DCE (10 ml) and DIPEA (0.23 ml) and added to the reaction mixture together with some activated 4A molsieves. After 1 h, ^{31}P NMR indicated formation of the activated ribosyl intermediates (δ = 98 & 94 ppm). Compound **3** (0.47 g, 1.0 mmol) was co-evaporated with dioxane (3x), dissolved in DCE (20 ml) and DIPEA (0.23 ml) and cooled to 0 °C. Activated 4A molsieves were added to the histidine solution followed by dropwise addition of the ribosyl intermediate using a syringe pump over 30 min. The reaction mixture was slowly warmed to rt overnight, diluted with DCM (50 ml) and washed with citric acid (1M, 80 ml) and brine (2x 50 ml). The H_2O fractions were back-extracted with DCM (80 ml) and the combined organic fractions were dried over $MgSO_4$, filtered and concentrated under reduced pressure. Purification

of the crude residue by silica gel column chromatography (DCM/MeOH = 100:0 → 98:2, 0.5% steps) provided a racemic mixture of title compound **9** (116 mg, 0.133 mmol, 27%) as a white foam and a single anomer (anomeric configuration not determined) of title compound **10** (52 mg, 0.060 mmol, 12%) as white foam.

9: $\mathbf{R_f}$ = 0.6 (DCM/MeOH = 95:5). **LC-MS** R_t = 8.38 min (10-90% MeCN/H_2O, TFA). **^{1}H NMR** (600 MHz, $CDCl_3$): δ 7.76 – 7.71 (m, 6H), 7.71 (s, 1H), 7.60 (dd, *J* = 7.6, 4.6 Hz, 6H), 7.55 (s, 2H), 7.38 – 7.19 (m, 66H), 7.21 – 7.07 (m, 6H), 6.91 (s, 1H), 6.63 (s, 2H), 6.54 (d, *J* = 8.0 Hz, 1H), 6.45 (d, *J* = 8.0 Hz, 2H), 5.69 (d, *J* = 5.3 Hz, 1H), 5.64 (d, *J* = 5.4 Hz, 2H), 5.18 – 5.06 (m, 6H), 4.71 – 4.40 (m, 18H), 4.40 – 4.17 (m, 16H), 4.11 (t, *J* = 5.1 Hz, 1H), 4.06 – 4.00 (m, 4H), 3.63 (dd, *J* = 10.6, 3.2 Hz, 2H), 3.56 (dd, *J* = 10.8, 3.2 Hz, 1H), 3.49 (ddd, *J* = 20.8, 10.7, 2.9 Hz, 3H), 3.16 – 2.96 (m, 6H). **^{13}C NMR** (151 MHz, $CDCl_3$): δ 171.7, 156.3, 156.3, 144.2, 144.2, 144.1, 144.0, 141.3, 141.3, 141.3, 137.9, 137.8, 137.5, 137.1, 137.0, 136.7, 136.0, 135.8, 135.8, 128.7, 128.6, 128.6, 128.6, 128.6, 128.6, 128.5, 128.3, 128.3, 128.2, 128.2, 128.1, 128.1, 128.1, 128.0, 127.9, 127.9, 127.7, 127.7, 127.7, 127.2, 127.1, 125.5, 125.5, 125.4, 125.4, 120.0, 119.9, 119.9, 117.0, 114.4, 88.9, 86.2, 82.4, 82.2, 81.9, 77.6, 76.8, 76.8, 73.7, 73.7, 73.2, 72.9, 72.8, 72.4, 69.9, 69.7, 67.3, 66.9, 66.9, 54.4, 54.2, 47.2, 30.0 **HRMS** $[C_{54}H_{51}N_3O_8 + H]^+$ = 870.37387 found, 870.37489 calculated.

10: $\mathbf{R_f}$ = 0.4 (DCM/MeOH = 95:5). **LC-MS** R_t = 8.33 min (10-90% MeCN/H_2O, TFA). **^{1}H NMR** (600 MHz, $CDCl_3$): δ 8.13 (s, 1H), 7.74 (d, *J* = 7.6 Hz, 2H), 7.55 – 7.50 (m, 2H), 7.41 – 7.14 (m, 22H), 7.08 (dd, *J* = 6.7, 2.8 Hz, 2H), 6.74 (s, 1H), 5.77 (d, *J* = 8.1 Hz, 1H), 5.75 (d, *J* = 5.5 Hz, 1H), 5.15 – 5.06 (m, 2H), 4.65 – 4.57 (m, 2H), 4.53 – 4.31 (m, 5H), 4.28 – 4.20 (m, 4H), 4.17 – 4.11 (m, 2H), 3.48 (dd, *J* = 10.9, 3.2 Hz, 1H), 3.41 (dd, *J* = 10.8, 3.2 Hz, 1H), 3.14 (dd, *J* = 15.6, 6.4 Hz, 1H), 3.00 (dd, *J* = 15.6, 5.9 Hz, 1H). **^{13}C NMR** (151 MHz, $CDCl_3$): δ 171.1, 155.9, 143.9, 143.7, 141.3, 141.3, 139.6, 137.8, 137.5, 136.9, 135.0, 128.7, 128.6, 128.5, 128.5, 128.5, 128.4, 128.1, 128.1, 128.0, 128.0, 127.8, 127.8, 127.7, 127.7, 127.1, 125.8, 125.2, 125.2, 120.0, 83.9, 81.9, 77.4, 76.7, 73.5, 73.3, 72.9, 69.5, 67.5, 67.2, 54.0, 47.1, 27.0. **HRMS** $[C_{54}H_{51}N_3O_8 + H]^+$ = 870.37381 found, 870.37489 calculated.

Fmoc-His (1′-N(τ)-2′,3′-bis-*O*-para-methoxybenzyl-5′-*O*-*tert*- diphenylsilyl- ribofuranosyl)-OBn (11) and Fmoc-His(1′-N(π)-2′,3′-bis-*O*-*para*-methoxybenzyl-5′-*O*-*tert*-diphenylsilyl-ribofuranosyl)-OBn (12).

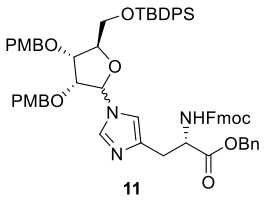

11

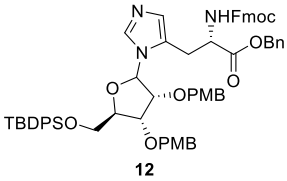

12

Bu_3PO (535 mg, 2.45 mmol) was co-evaporated with toluene (3x), dissolved in anhydrous DCE (10 ml) and cooled to 0 °C. Tf_2O (1 M, 1.15 ml, 1.15 mmol) was added dropwise over 20 min using a syringe pump and the resulting pinkish solution was stirred for 1 h at 0 °C. ^{31}P NMR indicated formation of the diphosphonium salt (δ = 119.5 ppm). **8** (0.31 g, 0.50 mmol) was co-evaporated with toluene (3x), dissolved in anhydrous DCE (10 ml) and DIPEA (0.23 ml) and added to the reaction mixture together with some activated 4Å molsieves. After 1 h, ^{31}P NMR indicated formation of the activated ribosyl intermediates (99 & 94 ppm). **5** (0.47 g, 1.0 mmol) was co-evaporated with dioxane (3x), dissolved in DCE (20 ml) and DIPEA (0.23 ml) and cooled to 0 °C. Activated 4Å molsieves were added to the histidine solution followed by dropwise addition of the ribosyl intermediate using a syringe pump over 30 min. The reaction mixture was slowly warmed to rt overnight, diluted with DCM (50 ml) and washed with citric acid (1M, 80 ml) and brine (2x 50 ml). The H_2O fractions were back-extracted with DCM (80 ml) and the combined organic fractions were dried over $MgSO_4$, filtered and concentrated under reduced pressure. Purification of the crude residue by silica gel column chromatography (DCM/MeOH = 100:0 → 98:2, 0.5% steps) provided an anomeric mixture (1:1.2 ratio, anomeric configuration not

determined) of title compound **11** (179 mg, 0.166 mmol, 33%) as a white foam and a single anomer (anomeric configuration not determined) of title compound **12** (0.10 g, 0.093 mmol, 18%) as clear oil.
11: R_f = 0.6 (DCM/MeOH = 97:3). **LC-MS** R_t = 10.22 min (10-90% MeCN/H_2O, TFA). **^{1}H NMR** (600 MHz, $CDCl_3$): δ 7.74 (s, 1H), 7.74 – 7.69 (m, 4.4H), 7.65 – 7.57 (m, 5.6H), 7.46 – 7.16 (m, 28.6H), 7.06 (dd, *J* = 8.5, 5.5 Hz, 4.4H), 6.95 (s, 1H), 6.89 – 6.77 (m, 8.8H), 6.71 – 6.67 (m, 2.4H), *6.61 (d, J = 8.0 Hz, 1H)*, 5.67 (d, *J* = 5.5 Hz, 1H), 5.65 (d, *J* = 6.3 Hz, 1H), 5.13 (d, *J* = 5.0 Hz, 4.4H), 4.71 (dt, *J* = 8.1, 5.2 Hz, 1H), 4.69 – 4.63 (m, 1.2H), 4.62 – 4.41 (m, 8.8H), 4.41 – 4.16 (m, 17.6H), 4.08 (dd, *J* = 5.1, 2.9 Hz, 1.2H), 3.98 (dd, *J* = 6.3, 5.1 Hz, 1.2H), 3.80 (dd, *J* = 11.5, 3.5 Hz, 1H), 3.78 – 3.68 (m, 14.2H), 3.66 (dd, *J* = 11.4, 2.9 Hz, 1.2H), 3.60 (dd, *J* = 11.5, 2.3 Hz, 1.2H), 3.20 – 3.09 (m, 2H), 3.11 – 2.97 (m, 2.4H), 1.02 (m, 19.8H). **^{13}C NMR** (151 MHz, $CDCl_3$): δ 171.5, 171.5, 159.4, 159.4, 159.4, 159.3, 156.2, 156.2, 144.0, 144.0, 143.9, 143.8, 141.1, 141.1, 141.1, 137.8, 136.4, 135.7, 135.6, 135.5, 135.4, 135.4, 132.8, 132.6, 132.5, 132.4, 130.0, 130.0, 129.9, 129.9, 129.6, 129.6, 129.4, 129.3, 129.3, 128.9, 128.8, 128.4, 128.4, 128.1, 128.0, 127.8, 127.8, 127.8, 127.5, 127.5, 127.5, 127.0, 127.0, 125.4, 125.3, 125.3, 125.2, 125.0, 125.0, 119.8, 119.8, 117.0, 114.3, 113.9, 113.8, 113.8, 113.8, 88.4, 86.2, 83.7, 83.5, 81.3, 77.4, 77.3, 76.0, 75.3, 72.6, 72.4, 72.2, 71.9, 67.1, 66.8, 66.7, 63.6, 63.6, 55.2, 55.1, 55.1, 55.1, 54.3, 54.1, 47.0, 26.8, 26.8, 26.8, 26.7, 19.1, 19.1. **HRMS** $[C_{65}H_{67}N_3O_{10}Si + H]^+$ = 1078.46628 found, 1078.46685 calculated.
12: R_f = 0.4 (DCM/MeOH = 97:3). **LC-MS** R_t = 10.22 min (10-90% MeCN/H_2O, TFA). **^{1}H NMR** (600 MHz, $CDCl_3$): δ 8.19 – 8.16 (m, 1H), 7.72 (d, *J* = 7.6 Hz, 2H), 7.60 – 7.44 (m, 6H), 7.40 – 7.18 (m, 17H), 7.01 (d, *J* = 8.6 Hz, 2H), 6.84 (d, *J* = 8.6 Hz, 2H), 6.75 (d, *J* = 8.7 Hz, 2H), 5.83 (d, *J* = 8.2 Hz, 1H), 5.69 (d, *J* = 5.7 Hz, 1H), 5.16 – 5.08 (m, 2H), 4.63 (dt, *J* = 8.2, 6.2 Hz, 1H), 4.58 (d, *J* = 11.5 Hz, 1H), 4.44 (d, *J* = 11.4 Hz, 1H), 4.37 – 4.17 (m, 6H), 4.13 (dd, *J* = 10.5, 7.4 Hz, 1H), 4.06 (d, *J* = 7.3 Hz, 1H), 3.81 – 3.66 (m, 7H), 3.58 (dd, *J* = 11.4, 2.8 Hz, 1H), 3.11 (dd, *J* = 15.7, 6.7 Hz, 1H), 3.00 (dd, *J* = 15.7, 5.7 Hz, 1H). **^{13}C NMR** (151 MHz, $CDCl_3$): δ 171.2, 159.4, 159.3, 155.9, 143.8, 143.7, 141.2, 141.2, 135.5, 135.5, 135.0, 132.8, 132.8, 129.9, 129.9, 129.7, 129.5, 128.9, 128.7, 128.6, 128.5, 128.4, 127.8, 127.8, 127.1, 127.1, 127.0, 125.8, 125.2, 125.1, 119.9, 113.9, 83.7, 83.4, 77.4, 76.1, 72.9, 72.5, 67.4, 67.1, 63.6, 55.3, 55.2, 53.8, 47.0, 26.9, 26.8, 19.2. **HRMS** $[C_{65}H_{67}N_3O_{10}Si + H]^+$ = 1078.46596 found, 1078.46685 calculated.

Fmoc-His(1'-N(τ)-2',3'-bis-*O* -para-methoxybenzyl-5'-*O* -*tert*-diphenylsilyl-ribofuranosyl)-OAllyl (13) and Fmoc-His(1'-α-N(π)-2',3'-bis-*O*-*para*-methoxybenzyl-5'-*O*-*tert*-diphenylsilyl-ribofuranosyl)-OAllyl (14).

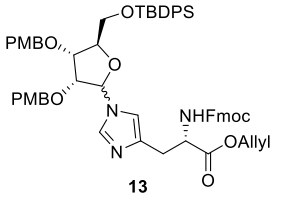

13

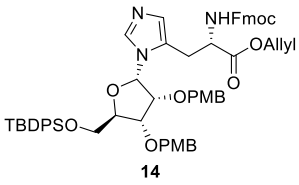

14

Bu_3PO (535 mg, 2.45 mmol) was co-evaporated with toluene (3x), dissolved in anhydrous DCE (10 ml) and cooled to 0 °C. Tf_2O (1 M, 1.15 ml, 1.15 mmol) was added dropwise over 20 min using a syringe pump and the resulting pinkish solution was stirred for 1 h at 0 °C. ^{31}P NMR indicated formation of the diphosphonium salt (δ = 119.5 ppm). **8** (0.31 g, 0.50 mmol) was co-evaporated with toluene (3x), dissolved in anhydrous DCE (10 ml) and DIPEA (0.23 ml) and added to the reaction mixture together with some activated 4Å molsieves. After 1 h, ^{31}P NMR indicated formation of the activated ribosyl intermediates (98 & 93 ppm). **5** (0.42 g, 1.0 mmol) was co-evaporated with dioxane (3x), dissolved in DCE (20 ml) and DIPEA (0.23 ml) and cooled to 0 °C. Activated 4Å molsieves were added to the histidine solution followed by dropwise addition of the ribosyl intermediate using a syringe pump over 30 min. The reaction mixture was slowly warmed to rt overnight, diluted with DCM (50 ml) and washed with citric acid (1M, 80 ml) and brine (2x 50 ml). The H_2O fractions were back-

extracted with DCM (80 ml) and the combined organic fractions were dried over $MgSO_4$, filtered and concentrated under reduced pressure. Purification of the crude residue by silica gel column chromatography (DCM/acetone = 100:0 → 90:10, 2.5% steps) provided an racemic mixture of title compound **13** (0.11 g, 0.11 mmol, 21%) as an off-white foam and title compound **14** (0.12 g, 0.12 mmol, 23%) an off-white foam.

13: $\mathbf{R_f}$ = 0.5 (DCM/MeOH = 95:5). **LC-MS** R_t = 9.28 min (10-90% MeCN/H_2O, TFA). **^{1}H NMR** (600 MHz, $CDCl_3$): δ 7.72 (t, *J* = 6.6 Hz, 5H), 7.64 – 7.57 (m, 13H), 7.45– 7.17 (m, 24H), 7.12 (s, 1H), 7.07 (dd, *J* = 21.9, 8.6 Hz, 4H), 6.88 – 6.77 (m, 9H), 6.61 (d, *J* = 8.0 Hz, 1H), 6.55 (d, *J* = 8.0 Hz, 1H), 5.88 – 5.79 (m, 2H), 5.71 (d, *J* = 5.6 Hz, 1H), 5.68 (d, *J* = 6.3 Hz, 1H), 5.29 – 5.13 (m, 4H), 4.70 – 4.32 (m, 13H), 4.31 – 4.16 (m, 11H), 4.09 (dd, *J* = 5.2, 2.9 Hz, 1H), 4.01 (t, *J* = 5.7 Hz, 1H), 3.76 (dd, *J* = 22.7, 11.9 Hz, 13H), 3.69 – 3.58 (m, 3H), 3.19 – 2.98 (m, 4H), 1.08 – 0.96 (m, 18H). **^{13}C NMR** (151 MHz, $CDCl_3$): δ 171.5, 171.4, 159.5, 159.5, 159.4, 156.3, 156.2, 144.1, 144.0, 144.0, 143.9, 141.2, 141.2, 141.2, 138.0, 136.6, 135.9, 135.6, 135.6, 135.5, 135.5, 135.5, 132.9, 132.7, 132.6, 132.5, 131.9, 131.8, 130.1, 130.0, 130.0, 129.9, 129.9, 129.7, 129.6, 129.5, 129.4, 129.4, 129.0, 128.9, 127.9, 127.9, 127.8, 127.8, 127.6, 127.6, 127.6, 127.6, 127.6, 127.1, 127.0, 125.4, 125.4, 125.3, 125.3, 119.9, 119.9, 119.8, 118.3, 118.2, 117.1, 114.2, 114.0, 114.0, 113., 113.9, 113.9, 88.4, 86.2, 83.8, 83.6, 81.4, 77.5, 76.1, 75.4, 72.7, 72.5, 72.3, 71.9, 67.1, 65.7, 65.7, 63.7, 63.7, 55.3, 55.2, 55.2, 55.2, 55.2, 54.3, 54.1, 47.1, 30.0, 29.9, 26.9, 26.9, 26.8, 19.2. **HRMS** $[C_{61}H_{65}N_3O_{10}Si + H]^+$ = 1028.45017 found, 1028.45120 calculated.

14: $\mathbf{R_f}$ = 0.4 (DCM/MeOH = 95:5). **LC-MS** R_t = 9.28 min (10-90% MeCN/H_2O, TFA). **^{1}H NMR** (600 MHz, $CDCl_3$): 8.19 (s, 1H), 7.71 (d, *J* = 7.6 Hz, 2H), 7.57 (d, *J* = 28.1 Hz, 2H), 7.52 – 7.46 (m, 4H), 7.41 – 7.28 (m, 8H), 7.28 – 7.18 (m, 4H), 7.04 (d, *J* = 8.6 Hz, 2H), 6.86 – 6.81 (m, 3H), 6.78 (d, *J* = 8.6 Hz, 2H), 5.88 – 5.77 (m, 2H), 5.72 (d, *J* = 5.7 Hz, 1H), 5.28 – 5.16 (m, 2H), 4.65 – 4.54 (m, 4H), 4.45 (d, *J* = 11.5 Hz, 1H), 4.39 – 4.29 (m, 3H), 4.25 (d, *J* = 11.5 Hz, 3H), 4.28 – 4.23 (m, 2H), 4.21 (q, *J* = 3.3 Hz, 1H), 4.17 (dd, *J* = 10.6, 7.4 Hz, 1H), 4.10 (t, *J* = 7.3 Hz, 1H), 3.79 – 3.69 (m, 7H), 3.60 (dd, *J* = 11.4, 2.8 Hz, 1H) 3.11 (dd, *J* = 15.6, 6.7 Hz, 1H), 3.01 (dd, *J* = 15.6, 5.8 Hz, 1H). **^{13}C NMR** (151 MHz, $CDCl_3$): δ 171.02, 159.46, 159.36, 155.87, 143.80, 143.74, 141.23, 135.56, 135.50, 132.87, 132.83, 131.36, 129.9, 129.8, 129.7, 129.5, 128.9, 127.8, 127.8, 127.8, 127.7, 127.6, 127.6, 127.0, 127.0, 125.8, 125.1, 125.1, 119.9, 119.1, 113.9, 113.8, 83.7, 83.4, 77.4, 76.1, 72.9, 72.5, 67.0, 66.2, 63.6, 55.2, 55.2, 53.7, 47.0, 26.8, 19.2. **HRMS** $[C_{61}H_{65}N_3O_{10}Si + H]^+$ = 1028.45031 found, 1028.45120 calculated.

Fmoc-His(1′-β-N(τ)-2′,3′-bis-*O*-para-methoxybenzyl-5′-*O*-*tert*-diphenylsilyl-ribofuranosyl)-OH (15) and Fmoc-His(1′-α-N(τ)-2′,3′-bis-*O*-para-methoxybenzyl-5′-*O*-*tert*-diphenylsilyl-ribofuranosyl)-OH (16).

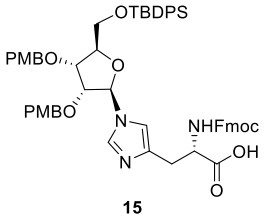

15

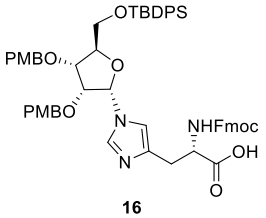

16

Method I: Compounds **11** (144 mg, 0.134 mmol) were dissolved in THF (7.5 ml) and cooled to 0 °C before adding a solution of LiOH (6.4 mg, 0.19 mmol) in H_2O (2.5 ml). After 1.5 h at 0 °C, the reaction mixture was diluted with DCM (50 ml) and washed with citric acid (10wt%, 2x 40 ml). The H_2O layer was back-extracted with DCM (2x 40 ml). The combined organic fractions were dried over $MgSO_4$, filtered and concentrated under reduced pressure. Purification of the crude residue by silica gel column chromatography (DCM/MeOH + 1% AcOH = 100:0 → 90:10) provided title compound **15** (30 mg, 0.030 mmol, 23%) as a white foam and **16** (32 mg, 0.030 mmol, 24%) as a white foam.

Method II: Compounds **13** (0.45 g, 0.44 mmol) and DMBA (82 mg, 0.52 mmol) were dissolved in anhydrous DCM (15 ml) and bubbled with argon gas for 10 min before adding $Pd(PPh_3)_4$ (15 mg, 0.013

mmol). The yellow solution was stirred for 1 h at rt, diluted with DCM (100 ml) and washed with citric acid (10wt%, 2x 100 ml). The H_2O layer was back-extracted with DCM (2x 50 ml). The combined organic fractions were dried over $MgSO_4$, filtered and concentrated under reduced pressure. Purification of the crude residue by silica gel column chromatography (DCM/MeOH + 1% AcOH = 100:0 → 95:5) provided title compound **15** (0.17 g, 0.17 mmol, 39%) as a white foam and **16** (0.17 g, 0.17 mmol, 39%) as a white foam.

15: $\mathbf{R_f}$ = 0.3 (DCM/MeOH + 1% AcOH = 95:5). **LC-MS** R_t = 6.78 min (50-90% MeCN/H_2O, TFA). **^{1}H NMR** (600 MHz, $CDCl_3$): δ 7.83 (s, 1H), 7.74 (d, *J* = 7.6 Hz, 2H), 7.60 – 7.50 (m, 6H), 7.41 – 7.26 (m, 10H), 7.20 (d, *J* = 8.6 Hz, 2H), 7.04 (d, *J* = 8.3 Hz, 2H), 6.87 – 6.84 (m, 3H), 6.77 (d, *J* = 8.6 Hz, 2H), 5.93 (d, *J* = 6.0 Hz, 1H), 5.65 (d, *J* = 6.3 Hz, 1H), 4.54 – 4.44 (m, 3H), 4.41 (d, *J* = 11.9 Hz, 1H), 4.37 (dd, *J* = 10.5, 7.3 Hz, 1H), 4.33 (d, *J* = 11.8 Hz, 1H), 4.23 – 4.15 (m, 3H), 4.02 – 3.99 (m, 1H), 3.96 (t, *J* = 5.7 Hz, 1H), 3.78 (s, 3H), 3.76 – 3.70 (m, 4H), 3.62 (dd, *J* = 11.6, 3.0 Hz, 1H), 3.32 (dd, *J* = 15.0, 2.9 Hz, 1H), 3.07 (dd, *J* = 15.1, 6.6 Hz, 1H), 0.98 (s, 9H). **^{13}C NMR** (214 MHz, $CDCl_3$): δ 173.2, 159.6, 159.5, 155.6, 144.1, 143.9, 141.3, 141.3, 135.6, 135.5, 134.5, 132.6, 132.5, 130.1, 130.1, 129.7, 129.5, 129.5, 129.4, 129.1, 128.7, 128.2, 127.9, 127.7, 127.7, 127.2, 127.1, 125.3, 120.0, 115.2, 114.1, 114.0, 114.0, 88.9, 84.2, 81.3, 75.5, 72.4, 72.1, 66.9, 63.6, 55.3, 55.2, 53.6, 47.2, 29.7, 29.7, 27.0, 26.9, 26.9, 19.2. **HRMS** $[C_{58}H_{61}N_3O_{10}Si + H]^+$ = 988.41908 found, 988.41990 calculated.

16: $\mathbf{R_f}$ = 0.2 (DCM/MeOH + 1% AcOH = 95:5). **LC-MS** R_t = 6.96 min (50-90% MeCN/H_2O, TFA). **^{1}H NMR** (600 MHz, $CDCl_3$): δ 8.15 (s, 1H), 7.72 (d, *J* = 7.7 Hz, 2H), 7.62 – 7.53 (m, 6H), 7.46 – 7.40 (m, 2H), 7.40 – 7.29 (m, 6H), 7.26 (t, *J* = 7.6 Hz, 2H), 7.11 (d, *J* = 8.1 Hz, 2H), 7.01 (s, 1H), 6.99 (d, *J* = 8.1 Hz, 2H), 6.80 (d, *J* = 8.2 Hz, 2H), 6.75 (d, *J* = 8.2 Hz, 2H), 6.12 (s, 1H), 5.60 (d, *J* = 5.7 Hz, 1H), 4.54 – 4.47 (m, 2H), 4.44 – 4.27 (m, 6H), 4.23 (s, 1H), 4.19 (t, *J* = 7.5 Hz, 1H), 4.14 – 4.10 (m, 1H), 3.73 (s, 3H), 3.71 – 3.66 (m, 4H), 3.54 (d, *J* = 11.6 Hz, 1H), 3.44 (d, *J* = 14.7 Hz, 1H), 3.23 (dd, *J* = 15.1, 6.4 Hz, 1H), 1.00 (s, 9H). **^{13}C NMR** (214 MHz, $CDCl_3$): δ 173.7, 159.6, 159.4, 155.7, 144.1, 144.1, 141.3, 141.3, 137.9, 136.0, 135.6, 135.5, 133.0, 132.8, 132.6, 130.0, 130.0, 129.6, 129.6, 129.5, 129.3, 129.1, 128.7, 128.3, 127.9, 127.9, 127.6, 127.1, 125.3, 125.3, 125.3, 119.9, 119.9, 118.0, 114.1, 113.9, 86.9, 84.9, 77.9, 77.3, 75.9, 73.0, 72.5, 66.7, 63.8, 55.3, 55.2, 54.0, 47.3, 26.9, 19.2. **HRMS** $[C_{58}H_{61}N_3O_{10}Si + H]^+$ = 988.41931 found, 988.41990 calculated.

Fmoc-His(1'-α-N(τ)-5'-*O-tert*-diphenylsilyl-ribofuranosyl)-OAllyl (17).

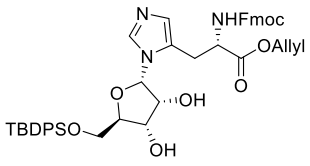

Compound **14** (0.17 g, 0.16 mmol) was dissolved in HFIP (3.3 ml) and cooled to 0 °C before adding HCl (0.2 M in HFIP, 0.33 ml). After 25 min, additional HCl (0.2 M in HFIP, 0.33 ml) was added and the resulting deep red solution was stirred for another 10 min. The reaction mixture was diluted with $NaHCO_3$ (sat., 30 ml) and extracted with DCM (3x 30 ml). The combined organic fractions were dried over $MgSO_4$, filtered and concentrated under reduced pressure. Purification of the crude residue by silica gel column chromatography (DCM/MeOH = 99:1 → 95:5) provided title compound **17** (46 mg, 0.058 mmol, 36%) as an off-white foam. $\mathbf{R_f}$ = 0.3 (DCM/MeOH = 90:10). **LC-MS** R_t = 8.00 min (10-90% MeCN/H_2O, TFA). **^{1}H NMR** (850 MHz, $CDCl_3$): δ 7.73 (s, 1H), 7.69 (d, *J* = 7.6 Hz, 2H), 7.64 (t, *J* = 7.5 Hz, 4H), 7.50 (d, *J* = 4.5 Hz, 1H), 7.41 – 7.30 (m, 8H), 7.26 – 7.21 (m, 2H), 6.66 (s, 1H), 6.11 (d, *J* = 8.0 Hz, 1H), 5.83 (d, *J* = 5.1 Hz, 1H), 5.82 – 5.75 (m, 1H), 5.26 (s, 1H), 5.24 (d, *J* = 17.1 Hz, 1H), 5.16 (d, *J* = 10.5 Hz, 1H), 4.60 – 4.55 (m, 3H), 4.53 (t, *J* = 5.6 Hz, 1H), 4.47 (t, *J* = 4.8 Hz, 1H), 4.35 – 4.30 (m, 2H), 4.21 (dd, *J* = 10.7, 7.4 Hz, 1H), 4.11 (t, *J* = 7.4 Hz, 1H), 3.83 (dd, *J* = 11.6, 3.1 Hz, 1H), 3.74 (dd, *J* = 11.6, 2.9 Hz, 1H), 3.13 (dd, *J* = 15.9, 5.6 Hz, 1H), 3.04 (dd, *J* = 15.8, 7.6 Hz, 1H), 1.04 (s, 9H). **^{13}C NMR** (214 MHz, $CDCl_3$): δ 171.1, 156.1, 143.8, 143.7, 141.2, 137.6, 135.6, 132.9, 132.9, 131.3, 129.9, 129.9, 127.9, 127.8, 127.8, 127.7, 127.1, 127.1, 126.6, 126.2, 125.2, 125.2, 120.0, 119.2, 86.7,

85.8, 72.3, 71.2, 67.2, 66.4, 64.2, 53.7, 53.5, 47.0, 26.9, 26.9, 26.9, 19.2. **HRMS** $[C_{45}H_{49}N_3O_8Si + H]^+$ = 788.33574 found, 788.33617 calculated.

Fmoc-His(1'-α-N(τ)-2',3'-bis-*O*-para-methoxybenzyl-5'-*O*-*tert*-diphenylsilyl-ribofuranosyl)-OH (18).

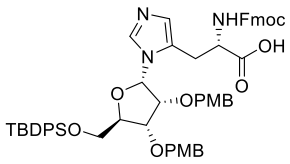

Method I: **12** (0.10 g, 0.093 mmol) was dissolved in THF (7.5 ml) and cooled to 0 °C before adding a solution of LiOH (4.4 mg, 0.19 mmol) in H_2O (2.5 ml). After 1.5 h at 0 °C, the reaction mixture was diluted with DCM (50 ml) and washed with HCl (1 M, 2x 50 ml). The H_2O layer was back-extracted with DCM (50 ml). The combined organic fractions were dried over $MgSO_4$, filtered and concentrated under reduced pressure. Purification of the crude residue by silica gel column chromatography (DCM/MeOH + 1% AcOH = 100:0 → 95:5) provided title compound **18** (43 mg, 0.044 mmol, 47%) as a white foam.

Method II: **14** (0.12 g, 0.12 mmol) and DMBA (31 mg, 0.20 mmol) were dissolved in anhydrous DCM (7.5 ml) and bubbled with argon gas for 10 min before adding $Pd(PPh_3)_4$ (13 mg, 0.012 mmol). The yellow solution was stirred for 30 min at rt, diluted with DCM (40 ml) and washed with citric acid (10wt%, 2x 40 ml). The water layer was back-extracted with DCM (2x 40 ml). The combined organic fractions were dried over $MgSO_4$, filtered and concentrated under reduced pressure. Purification of the crude residue by silica gel column chromatography (DCM/MeOH + 1% AcOH = 100:0 → 90:10) provided title compound **18** (0.10 g, 0.10 mmol, 89%) as an off-white foam.

$\mathbf{R_f}$ = 0.20 (DCM/MeOH + 1% AcOH = 95:5). **LC-MS** R_t = 8.70 min (10-90% MeCN/H_2O, TFA). **^{1}H NMR** (850 MHz, Acetone): δ 8.51 (s, 1H), 7.80 – 7.57 (m, 8H), 7.46 – 7.11 (m, 15H), 6.82 (dd, *J* = 57.5, 8.3 Hz, 4H), 6.33 (s, 1H), 4.69 – 4.07 (m, 11H), 3.79 – 3.59 (m, 8H), 3.44 – 3.39 (m, 1H), 3.33 – 3.24 (m, 1H), 0.99 (s, 9H). **^{13}C NMR** (214 MHz, Acetone): δ 174.2, 160.2, 160.2, 156.8, 144.9, 144.8, 141.9, 138.4, 136.2, 136.2, 135.5, 133.8, 133.6, 130.6, 130.6, 130.5, 130.3, 130.2, 129.4, 128.6, 128.3, 127.9, 126.1, 126.1, 124.5, 120.6, 114.5, 114.5, 85.3, 84.4, 78.1, 76.9, 73.3, 72.6, 67.2, 64.3, 55.4, 55.4, 54.9, 47.8, 27.2, 19.6. **HRMS** $[C_{58}H_{61}N_3O_{10}Si + H]^+$ = 988.42016 found, 988.41990 calculated.

β-N(τ)-ADPr-His: TF[H]^{ADPr}GAGLVVPVDK (25).

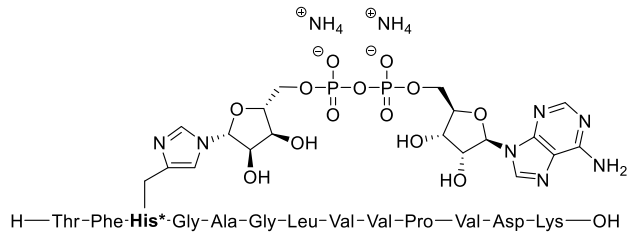

Title compound **25** was synthesized according to the general resin based procedure described above on a 50 µmol scale by incorporating the β-N(τ)-ADP-ribosylated histidine **15**. Purification of half of the crude residue (25 µmol) by preparative HPLC (NH_4OAc buffer) and subsequent lyophilization yielded title compound **25** (13.0 mg, 6.93 µmol, 28%) as a fluffy white powder. **LC-MS** R_t = 4.29 min (10-50% MeCN/H_2O, TFA). **^{1}H NMR** (400 MHz, D_2O): δ 8.73 (d, *J* = 1.6 Hz, 1H), 8.44 (s, 1H), 8.17 (s, 1H), 7.42 (s, 1H), 7.25 – 7.14 (m, 3H), 7.12 (d, *J* = 7.2 Hz, 2H), 6.03 (d, *J* = 5.7 Hz, 1H), 5.74 (d, *J* = 4.5 Hz, 1H). $[C_{77}H_{119}N_{21}O_{30}P_2 + 3H]^{3+}$ = 627.60438 found, 627.60417 calculated.

α-N(τ)-ADPr-His: TF[H]^{ADPr}GAGLVVPVDK (26).

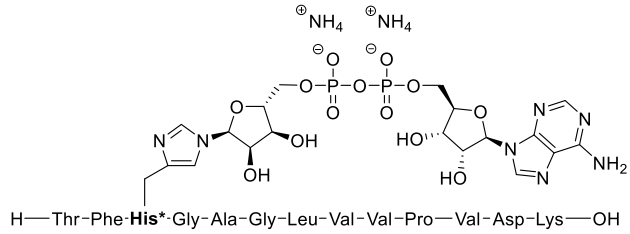

Title compound **26** was synthesized according to the general resin based procedure described above on a 50 µmol scale by incorporating the α-N(τ)-ADP-ribosylated histidine **16**. Purification of half of the crude residue (25 µmol) by preparative HPLC (AcOH buffered) and subsequent lyophilization yielded title compound **26** (16.2 mg, 8.62 µmol, 35%) as a fluffy white powder. **LC-MS** R_t = 4.26 min (10-50% MeCN/H_2O, TFA). **^{1}H NMR** (400 MHz, D_2O): δ 8.64 (s, 1H), 8.48 (s, 1H), 8.19 (s, 1H), 7.30 (s, 1H), 7.27 – 7.21 (m, 3H), 7.15 (d, *J* = 6.2 Hz, 2H), 6.07 (d, *J* = 6.1 Hz, 1H), 6.04 (d, *J* = 5.3 Hz, 1H). **^{31}P NMR** (162 MHz, D_2O): δ -10.41, -10.54, -10.71, -10.84. **HRMS** $[C_{77}H_{119}N_{21}O_{30}P_2 + 2H]^{2+}$ = 940.90222 found, 940.90262 calculated; $[C_{77}H_{119}N_{21}O_{30}P_2 + 3H]^{3+}$ = 627.60418 found, 627.60417 calculated.

α-N(π)-ADPr-His: TF[H]^{ADPr}GAGLVVPVDK (27).

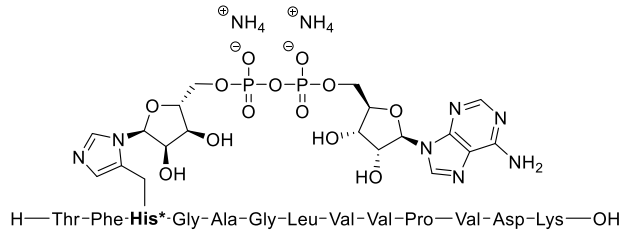

Title compound **27** was synthesized according to the general resin based procedure described above on a 50 µmol scale by incorporating the N(π)-ADP-ribosylated histidine **18**. Purification of half of the crude residue (25 µmol) by preparative HPLC (AcOH buffered) and subsequent lyophilization yielded title compound **27** (12.9 mg, 6.91 µmol, 28%) as a fluffy white powder. **LC-MS** R_t = 4.24 min (10-50% MeCN/H_2O, TFA). **^{1}H NMR** (400 MHz, D_2O): δ 8.68 (s, 1H), 8.47 (s, 1H), 8.17 (s, 1H), 7.28 – 7.21 (m, 3H), 7.16 (d, *J* = 7.4 Hz, 2H), 7.05 (s, 1H), 6.12 (d, *J* = 5.2 Hz, 1H), 6.05 (d, *J* = 6.0 Hz, 1H).**^{31}P NMR** (162 MHz, D_2O): δ -10.47, -10.60, -10.69, -10.82. **HRMS** $[C_{77}H_{119}N_{21}O_{30}P_2 + 2H]^{2+}$ = 940.90226 found, 940.90262 calculated; $[C_{77}H_{119}N_{21}O_{30}P_2 + 3H]^{3+}$ = 627.60421 found, 627.60417 calculated.

References

1. Ramazi, S. & Zahiri, J. Post-translational modifications in proteins: resources, tools and prediction methods. *Database* **2021**, baab012 (2021).
2. Choudhary, C. *et al.* Lysine Acetylation Targets Protein Complexes and Co-Regulates Major Cellular Functions. *Science* **325**, 834–840 (2009).
3. Nsiah-Sefaa, A. & McKenzie, M. Combined defects in oxidative phosphorylation and fatty acid β-oxidation in mitochondrial disease. *Biosc. Rep.* **36**, e00313 (2016).
4. Karve, T. M. & Cheema, A. K. Small changes huge impact: the role of protein posttranslational modifications in cellular homeostasis and disease. *J. Amino Acids* (2011).
5. Popovic, D., Vucic, D. & Dikic, I. Ubiquitination in disease pathogenesis and treatment. *Nat Med* **20**, 1242–1253 (2014).
6. Chambon, P., Weill, J. D., Doly, J., Strosser, M. T. & Mandel, P. On the formation of a novel adenylic compound by enzymatic extracts of liver nuclei. *Biochem. Biophys. Res. Commun.* **25**, 638–643 (1966).
7. Okayama, H., Edson, C. M., Fukushima, M., Ueda, K. & Hayaishi, O. Purification and properties of poly(adenosine diphosphate ribose) synthetase. *J. Biol. Chem.* **252**, 7000–7005 (1977).
8. Lüscher, B. *et al.* ADP-ribosyltransferases, an update on function and nomenclature. *FEBS J.* (2021) doi:10.1111/febs.16142.
9. Miwa, M. *et al.* A 13C NMR study of poly(adenosine diphosphate ribose) and its monomers: evidence of alpha-(1″ leads to 2′) ribofuranosy1 ribofuranoside risidue. *Nucleic Acids Res* **4**, 3997–4005 (1977).
10. Juarez-Salinas, H., Levi, V., Jacobson, E. L. & Jacobson, M. K. Poly(ADP-ribose) has a branched structure in vivo. *J. Biol. Chem.* **257**, 607–609 (1982).
11. Lin, W., Amé, J.-C., Aboul-Ela, N., Jacobson, E. L. & Jacobson, M. K. Isolation and Characterization of the cDNA Encoding Bovine Poly(ADP-ribose) Glycohydrolase. *J. Biol. Chem.* **272**, 11895–11901 (1997).
12. Slade, D. *et al.* The structure and catalytic mechanism of a poly(ADP-ribose) glycohydrolase. *Nature* **477**, 616–620 (2011).
13. Jankevicius, G. *et al.* A family of macrodomain proteins reverses cellular mono-ADP-ribosylation. *Nat. Struct,. Mol. Biol.* **20**, 508–514 (2013).
14. Rosenthal, F. *et al.* Macrodomain-containing proteins are new mono-ADP-ribosylhydrolases. *Nat. Struct. Mol. Biol.* **20**, 502–507 (2013).
15. Moss, J., Tsai, S. C., Adamik, R., Chen, H. C. & Stanley, S. J. Purification and characterization of ADP-ribosylarginine hydrolase from turkey erythrocytes. *Biochemistry* **27**, 5819–5823 (1988).
16. Fontana, P. *et al.* Serine ADP-ribosylation reversal by the hydrolase ARH3. *Elife* **6**, e28533 (2017).
17. Oppenheimer, N. J. Structural determination and stereospecificity of the choleragen-catalyzed reaction of NAD+ with guanidines. *J. Biol. Chem.* **253**, 4907–4910 (1978).
18. Cassel, D. & Pfeuffer, T. Mechanism of cholera toxin action: Covalent modification of the guanyl nucleotide-binding protein of the adenylate cyclase system. *Proc. Natl. Acad. Sci.* **75**, 2669–2673 (1978).
19. West, R. E., Moss, J., Vaughan, M., Liu, T. & Liu, T. Y. Pertussis toxin-catalyzed ADP-ribosylation of transducin. Cysteine 347 is the ADP-ribose acceptor site. *J. Biol. Chem.* **260**, 14428–14430 (1985).
20. Robinson, E. A., Henriksen, O. & Maxwell, E. S. Elongation Factor 2 AMINO ACID SEQUENCE AT THE SITE OF ADENOSINE DIPHOSPHATE RIBOSYLATION. *J. Biol. Chem.* **249**, 5088–5093 (1974).
21. Ness, B. G. V., Howard, J. B. & Bodley, J. W. ADP-ribosylation of elongation factor 2 by diphtheria toxin. NMR spectra and proposed structures of ribosyl-diphthamide and its hydrolysis products. *J. Biol. Chem.* **255**, 10710–10716 (1980).
22. Zhang, Y., Wang, J., Ding, M. & Yu, Y. Site-specific characterization of the Asp- and Glu-ADP-ribosylated proteome. *Nat Methods* **10**, 981–984 (2013).
23. Huang, D. *et al.* Functional Interplay between Histone H2B ADP-Ribosylation and Phosphorylation Controls Adipogenesis. *Mol. Cell* **79**, 934-949.e14 (2020).
24. Altmeyer, M., Messner, S., Hassa, P. O., Fey, M. & Hottiger, M. O. Molecular mechanism of poly(ADP-ribosyl)ation by PARP1 and identification of lysine residues as ADP-ribose acceptor sites. *Nucleic Acids Res* **37**, 3723–3738 (2009).
25. Leidecker, O. *et al.* Serine is a new target residue for endogenous ADP-ribosylation on histones. *Nat. Chem. Biol.* **12**, 998–1000 (2016).
26. Larsen, S. C., Hendriks, I. A., Lyon, D., Jensen, L. J. & Nielsen, M. L. Systems-wide Analysis of Serine ADP-Ribosylation Reveals Widespread Occurrence and Site-Specific Overlap with Phosphorylation. *Cell Rep.* **24**, 2493-2505.e4 (2018).
27. Bartlett, E. *et al.* Interplay of Histone Marks with Serine ADP-Ribosylation. *Cell Rep.* **24**, 3488-3502.e5 (2018).
28. Buch-Larsen, S. C., Rebak, A. K. L. F. S., Hendriks, I. A. & Nielsen, M. L. Temporal and Site-Specific ADP-Ribosylation Dynamics upon Different Genotoxic Stresses. *Cells* **10**, 2927 (2021).
29. Bonfiglio, J. J. *et al.* Serine ADP-Ribosylation Depends on HPF1. *Mol. Cell* **65**, 932-940.e6 (2017).
30. Brustel, J. *et al.* Linking DNA repair and cell cycle progression through serine ADP-ribosylation of histones. *Nat. Commun.* **13**, 185 (2022).

31. Fehr, A. R. *et al.* The impact of PARPs and ADP-ribosylation on inflammation and host–pathogen interactions. *Genes Dev.* **34**, 341–359 (2020).
32. Mashimo, M., Kato, J. & Moss, J. ADP-ribosyl-acceptor hydrolase 3 regulates poly (ADP-ribose) degradation and cell death during oxidative stress. *Proc. Natl. Acad. Sci.* **110**, 18964–18969 (2013).
33. Kharadia, S. V. & Graves, D. J. Relationship of phosphorylation and ADP-ribosylation using a synthetic peptide as a model substrate. *J. Biol. Chem.* **262**, 17379–17383 (1987).
34. Bhogaraju, S. *et al.* Phosphoribosylation of Ubiquitin Promotes Serine Ubiquitination and Impairs Conventional Ubiquitination. *Cell* **167**, 1636-1649.e13 (2016).
35. Voorneveld, J. *et al.* Arginine ADP-Ribosylation: Chemical Synthesis of Post-Translationally Modified Ubiquitin Proteins. *J. Am. Chem. Soc.* **144**, 20582–20589 (2022).
36. Danhauser, K. *et al.* Bi-allelic ADPRHL2 Mutations Cause Neurodegeneration with Developmental Delay, Ataxia, and Axonal Neuropathy. *J. Hum. Genet.* **103**, 817–825 (2018).
37. Szántó, M. & Bai, P. The role of ADP-ribose metabolism in metabolic regulation, adipose tissue differentiation, and metabolism. *Genes Dev.* **34**, 321–340 (2020).
38. Moyle, P. M. & Muir, T. W. Method for the Synthesis of Mono-ADP-ribose Conjugated Peptides. *J. Am. Chem. Soc.* **132**, 15878–15880 (2010).
39. Kistemaker, H. A. V. *et al.* Synthesis and Macrodomain Binding of Mono-ADP-Ribosylated Peptides. *Angew. Chem. Int. Ed.* **55**, 10634–10638 (2016).
40. Voorneveld, J. *et al.* Synthetic α- and β-Ser-ADP-ribosylated Peptides Reveal α-Ser-ADPr as the Native Epimer. *Org. Lett.* **20**, 4140–4143 (2018).
41. Minnee, H. *et al.* Mimetics of ADP-Ribosylated Histidine through Copper(I)-Catalyzed Click Chemistry. *Org. Lett.* **24**, 3776–3780 (2022).
42. Voorneveld, J. *et al.* Molecular Tools for the Study of ADP-Ribosylation: A Unified and Versatile Method to Synthesise Native Mono-ADP-Ribosylated Peptides. *Chem. Eur. J.* **27**, 10621–10627 (2021).
43. Bonfiglio, J. J. *et al.* An HPF1/PARP1-Based Chemical Biology Strategy for Exploring ADP-Ribosylation. *Cell* **183**, 1086-1102.e23 (2020).
44. van der Heden van Noort, G. J., van der Horst, M. G., Overkleeft, H. S., van der Marel, G. A. & Filippov, D. V. Synthesis of Mono-ADP-Ribosylated Oligopeptides Using Ribosylated Amino Acid Building Blocks. *J. Am. Chem. Soc.* **132**, 5236–5240 (2010).
45. Kaplan, N. O. & Ciotti, M. M. CHEMISTRY AND PROPERTIES OF THE 3-ACETYLPYRIDINE ANALOGUE OF DIPHOSPHOPYRIDINE NUCLEOTIDE. *J. Biol. Chem.* **221**, 823–832 (1956).
46. Walter, P. & Kaplan, N. O. Substituted Nicotinamide Analogues of Nicotinamide Adenine Dinucleotide. *J. Biol. Chem.* **238**, 2823–2830 (1963).
47. Tono-oka, S. *et al.* Enzymic Synthesis and Biochemical Activity of Various Indazole Adenine Dinucleotides. *BCSJ* **58**, 309–315 (1985).
48. Tono-Oka, S. & Azuma, I. Enzymatic Preparations and Regiochemical Properties of Some New ADP- Ribosylated 1,2,4-Triazoles. *ChemInform* **22**, (1991).
49. Tono-oka, S. *et al.* Evidence for Enzymatic ADP-Ribosylation to Histidine and Related Dipeptides. *Acta Chem. Scand.* **48**, 780–782 (1994).
50. Al Mourabit, A., Beckmann, M., Poupat, C., Ahond, A. & Potier, P. New C2 symmetrical and semisymmetrical substituted imidazolium ribonucleoside. Imidazolic nucleosides analogues. *Tetrahedron: Asymmetry* **7**, 3455–3464 (1996).
51. Seley, K. L., Salim, S. & Zhang, L. "Molecular Chameleons". Design and Synthesis of C-4-Substituted Imidazole Fleximers. *Org. Lett.* **7**, 63–66 (2005).
52. Li, D., Bao, H., Tan, Q., Cai, D. & You, T. Synthesis of Ribavirin Analogues Containing Amino-Acid Residues. *Synth. Commun.* **35**, 1017–1026 (2005).
53. Hensel, S., Megger, N., Schweizer, K. & Müller, J. Second generation silver(I)-mediated imidazole base pairs. *Beilstein J. Org. Chem.* **10**, 2139–2144 (2014).
54. Miyake, T., Tsuchiya, T., Umezawa, S., Saito, S. & Umezawa, H. Studies on Glycosylation of erythro-β-Hydroxy-L-histidine. A Key Step of Bleomycin Total Synthesis. *BCSJ* **59**, 1387–1395 (1986).
55. McLachlan, M. M. W. & Taylor, C. M. Construction of a τ-galactosyl histidine moiety. *Tetrahedron Lett.* **39**, 3055–3056 (1998).
56. Hendriks, I. A., Larsen, S. C. & Nielsen, M. L. An advanced strategy for comprehensive profiling of ADP-ribosylation sites using mass spectrometry-based proteomics. *Mol. Cell Proteomics* **18**, 1010–1026 (2019).
57. Gold, H. *et al.* Synthesis of Sugar Nucleotides by Application of Phosphoramidites. *J. Org. Chem.* **73**, 9458–9460 (2008).
58. Hananya, N., Daley, S. K., Bagert, J. D. & Muir, T. W. Synthesis of ADP-Ribosylated Histones Reveals Site-Specific Impacts on Chromatin Structure and Function. *J. Am. Chem. Soc.* **143**, 10847–10852 (2021).
59. Voorneveld, J. *et al.* Molecular Tools for the Study of ADP-Ribosylation: A Unified and Versatile Method to Synthesise Native Mono-ADP-Ribosylated Peptides. *Chem. Eur. J.* **27**, 10621–10627 (2021).
60. Zhao, X. Z., Hymel, D. & Burke, T. R. Application of oxime-diversification to optimize ligand interactions within a cryptic pocket of the polo-like kinase 1 polo-box domain. *Bioorg. Med. Chem. Lett.* **26**, 5009–5012 (2016).
61. Mukaiyama, T. & Suda, S. Diphosphonium Salts as Effective Reagents for Stereoselective Synthesis of 1,2-cis-Ribofuranosides. *Chem. Lett.* **19**, 1143–1146 (1990).

62. van der Heden van Noort, G. J., Overkleeft, H. S., van der Marel, G. A. & Filippov, D. V. Ribosylation of Adenosine: An Orthogonally Protected Building Block for the Synthesis of ADP-Ribosyl Oligomers. *Org. Lett.* **13**, 2920–2923 (2011).
63. van Rijssel, E. R. *et al.* Furanosyl Oxocarbenium Ion Stability and Stereoselectivity. *Angew. Chem. Int. Ed.* **53**, 10381–10385 (2014).
64. Koźmiński, W. & Nanz, D. HECADE: HMQC- and HSQC-Based 2D NMR Experiments for Accurate and Sensitive Determination of Heteronuclear Coupling Constants from E.COSY-Type Cross Peaks. *J. Magn. Reson.* **124**, 383–392 (1997).
65. Napolitano, J. G. *et al.* On the Configuration of Five-Membered Rings: A Spin–Spin Coupling Constant Approach. *Chem. Eur. J.* **17**, 6338–6347 (2011).
66. Volbeda, A. G. *et al.* Chemoselective Cleavage of p-Methoxybenzyl and 2-Naphthylmethyl Ethers Using a Catalytic Amount of HCl in Hexafluoro-2-propanol. *J. Org. Chem.* **80**, 8796–8806 (2015).
67. Bourne, E. J., Finch, P. & Nagpurkar, A. G. The synthesis and hydrolytic stability of 1-glucopyranosylimidazoles. *J. Chem. Soc., Perkin Trans. 1* 2202–2205 (1972) doi:10.1039/P19720002202.
68. Rack, J. G. M., Palazzo, L. & Ahel, I. (ADP-ribosyl)hydrolases: structure, function, and biology. *Genes Dev.* **34**, 263–284 (2020).
69. Tromans-Coia, C. *et al.* TARG1 protects against toxic DNA ADP-ribosylation. *Nucleic Acids Res.* **49**, 10477–10492 (2021).
70. Schuller, M. *et al.* Molecular basis for DarT ADP-ribosylation of a DNA base. *Nature* **596**, 597–602 (2021).
71. Schuller, M. *et al.* Molecular basis for the reversible ADP-ribosylation of guanosine bases. *Molecular Cell* **83**, 2303-2315.e6 (2023).
72. Palazzo, L. *et al.* Processing of protein ADP-ribosylation by Nudix hydrolases. *Biochem.* **468**, 293–301 (2015).
73. Minnee, H. *et al.* Mimetics of ADP-Ribosylated Histidine through Copper(I)-Catalyzed Click Chemistry. *Org. Lett.* **24**, 3776–3780 (2022).
74. Stevens, L. A. *et al.* The ARH and Macrodomain Families of α-ADP-ribose-acceptor Hydrolases Catalyze α-NAD+ Hydrolysis. *ACS Chem. Biol.* **14**, 2576–2584 (2019).
75. Oka, S., Kato, J. & Moss, J. Identification and Characterization of a Mammalian 39-kDa Poly(ADP-ribose) Glycohydrolase *. *J. Biol. Chem.* **281**, 705–713 (2006).
76. Ono, T., Kasamatsu, A., Oka, S. & Moss, J. The 39-kDa poly(ADP-ribose) glycohydrolase ARH3 hydrolyzes O-acetyl-ADP-ribose, a product of the Sir2 family of acetyl-histone deacetylases. *Proc. Natl. Acad. Sci.* **103**, 16687–16691 (2006).
77. Munnur, D. & Ahel, I. Reversible mono-ADP-ribosylation of DNA breaks. *FEBS J.* **284**, 4002–4016 (2017).